SIAM J. Applied Dynamical Systems
Vol. 15, No. 1, pp. 287–321

R_0 Analysis of a Benthic-Drift Model for a Stream Population*

Qihua Huang†, Yu Jin‡, and Mark A. Lewis§

Abstract. One key issue for theory in stream ecology is how much stream flow can be changed while still maintaining an intact stream ecology, instream flow needs (IFNs); the study of determining IFNs is challenging due to the complex and dynamic nature of the interaction between the stream environment and the biological community. We develop a process-oriented benthic-drift model that links changes in the flow regime and habitat availability with population dynamics. In the model, the stream is divided into two zones, drift zone and benthic zone, and the population is divided into two interacting compartments, individuals residing in the benthic zone and individuals dispersing in the drift zone. We study the population persistence criteria, based on the net reproductive rate R_0 and on related measures. We develop new theory to calculate these quantities and use them to investigate how the various flow regimes, population birth rate, individual transfer rates between zones, and river heterogeneity affect population persistence. The theory developed here provides the basis for effective decision-making tools for water managers.

Key words. benthic-drift model, next generation operator, persistence, net reproductive rate, river heterogeneity

AMS subject classifications. 35K10, 47A75, 92B05

DOI. 10.1137/15M1014486

1. Introduction.

A large number of organisms live in environments that are characterized by a predominately unidirectional flow such as streams and rivers. One key issue for theory in stream ecology, which has been termed the "drift paradox," is how a population can persist in rivers despite the flow-induced washout. The analogous issue in coastal marine systems is population persistence and distribution in the presence of long-shore currents. Although the problem has been recognized for almost half a century, and despite considerable efforts in documenting drift in the field, it has not received theoretical attention until the last decade. In recent years, in the study of the drift paradox, mathematical models such as partial differential equations, integro-difference equations, and integro-differential equations, have been used to understand the effect of population demography, individual movement, and flow dynamics on the spread and persistence of a population in streams and rivers.

*Received by the editors March 30, 2015; accepted for publication (in revised form) by J. Sneyd December 7, 2015; published electronically February 9, 2016.
http://www.siam.org/journals/siads/15-1/M101448.html

†Center for Mathematical Biology, Department of Mathematical and Statistical Sciences, University of Alberta, Edmonton, AB, T6G 2G1, Canada (qihua@ualberta.ca). The work of this author was supported by the Alberta Environment and Sustainable Resource Development and the Alberta Water Research Institute.

‡Department of Mathematics, University of Nebraska-Lincoln, Lincoln, NE, 68588 (yjin6@unl.edu). The work of this author was supported by an AMS-Simons Travel grant and NSF Grant DMS 1411703.

§Center for Mathematical Biology, Department of Mathematical and Statistical Sciences, University of Alberta, Edmonton, AB, T6G 2G1, Canada, and Department of Biological Sciences, University of Alberta, Edmonton, AB, T6G 2E9, Canada (mark.lewis@ualberta.ca). The work of this author was supported by a Canada Research Chair, NSERC Discovery and Accelerator grants, and a Killam Research Fellowship.

Another key issue for stream ecology is what kind of flows are needed to maintain an intact stream ecology. This is referred to as instream flow needs (INFs). Fresh water is a limited and precious resource. Increasing and conflicting demands for freshwater resources make it necessary to evaluate IFNs in streams and rivers. If natural flow regimes change (e.g., due to anthropogenic influence), this can directly impact the ecology of organisms inhabiting the stream and river habitats. Assessing population and community persistence for varying stream flows therefore is a key issue for biodiversity maintenance in advective environments.

Determining IFNs is challenging due to the complex and dynamic nature of the interaction between the stream environment and the biological community. Resource managers have traditionally relied on simple hydrological and habitat-association methods to predict how changes in river flow regimes will affect the viability of instream populations and communities. These methods often account only for the dynamics nature of hydrology and physical habitat: biological components of ecosystems are treated as a static response variable to this dynamics physical environment. Ecologists have advocated an alternative method: process-oriented ecological models that link changes in the flow regime and habitat availability with population dynamics [2]. Such models allow consideration of external forcing by the physical environment, as well as feedbacks between biotic and abiotic components.

In recent work, stemming from interests in the "drift paradox" and IFNs, Mckenzie et al. [22] developed a process-oriented ecological model that couples population dynamics of river communities to the hydraulic dynamics of a river. The model is an advection-diffusion-reaction equation that describes the dynamics of a single population undergoing continuous growth and dispersal in a stream:

$$\frac{\partial N}{\partial t} = g(x,N)N - \frac{Q}{A(x)}\frac{\partial N}{\partial x} + \frac{1}{A(x)}\frac{\partial}{\partial x}\left(D(x)A(x)\frac{\partial N}{\partial x}\right), \tag{1.1}$$

where $N(x,t)$ is the density of the population per unit volume at location x and time t, $g(x,N)$ is the per capita growth rate function, A is the cross-sectional area of the stream, D is the spatially variable diffusion coefficient, and Q is the constant stream discharge. By adapting three measures of population persistence, proposed by [19], Mckenzie et al. studied related population persistence measures in rivers under various flow regimes. The three measures are connected through the next generation operator, which maps the population from one generation to its offspring in the next generation. As spatial reaction-advection-diffusion equations fall under the broader category of infinite-dimensional dynamical systems, Mckenzie et al. applied the theory of Thieme [29] for R_0 in infinite-dimensional dynamical systems to present their mathematical framework. The mathematical methods were then applied to analyze IFNs for populations in rivers.

In this work, we extend the model (1.1) to a benthic-drift model by partitioning the river into two zones, drift zone and benthic zone and dividing the population into two interacting compartments, individuals residing in the benthic zone and individuals dispersing in the drift zone. Our extension is motivated by the following facts: (1) Hydrologically, stream hydraulic characteristics are important in the ecology of streams. Of particular importance is the presence of free-flowing water zones on the top and transient storage zones along the bottom. In the storage zones, water movement can be approximated as zero flow [4, 7, 23, 30]. The bottom friction, especially from irregularities such as rocks, create these areas of near zero-flow

water. In addition, interstitial waters in sediments or within algal mats, backwater areas, and pools can also act as transient storage zones [4, 23, 30]. Storage zones are also places where the nutrient cycling regime in the biological community is likely to be quite different from that in the free-flowing part of the stream [7]. (2) Ecologically, many aquatic organisms reside mainly in the storage zone but move by jumping into the free-flowing zone and drifting downstream [1]. Moreover, the switching rates of individuals between the benthos and the drifting water may be determined by organism behavior rather than by stream hydrodynamics. For example, there is evidence that the switching rates can depend on the organisms response to environmental factors such as food abundance and density dependence [1, 11, 25].

We are concerned with the persistence criteria for a population living in a benthos-drifting water environment. To this end, we extend the three measures of population persistence, initially presented for the single compartment model (1.1) in [22], to a benthic-drift model. The mathematical theory and methods are then applied to our scientific goal: to provide a new way of analyzing IFN for populations in rivers.

The first measure of persistence describes the *fundamental niche* of the population and we denote it $R_{\text{loc}}(x)$. It is the product of reproduction and survival at the location x and represents local population persistence. That is, in the absence of dispersal, a population will persist at the location if $R_{\text{loc}}(x) > 1$ but will not persist if $R_{\text{loc}}(x) < 1$. In this work, we use $R_{\text{loc}}(x)$ to answer the following question: if an individual is placed at location x of the benthic zone and it does not move, what will its lifetime reproductive output at that location be?

The second measure of persistence describes the *source-sink distribution* and is denoted by $R_\delta(x)$. It represents lifetime reproductive output of an individual initially introduced at x, undergoing survival, reproduction, and dispersal. Locations where $R_\delta(x) > 1$ function as sources because individuals at location x on average produce more than one offspring in the whole spatial domain. Locations where $R_\delta(x) < 1$ function as sinks because on average the lifetime reproductive output of an individual introduced at location x is less than one offspring. In this work, we use $R_\delta(x)$ to answer the following question: if an individual is introduced at location x in the benthic zone and undergoes continuous dispersal in the drift zone and reproduction in the benthic zone, what will its lifetime reproductive output be?

Although R_{loc} can describe local dynamics such as fundamental niche, and $R_\delta(x)$ describes source and sink distributions in the spatial habitat, they do not inform us about the global persistence or extinction of a population. To investigate this we turn to the final measure of persistence, the *net reproductive rate*, R_0, which is defined mathematically as the spectral radius of the next generation operator. Biologically, it can be interpreted as the average number of offspring produced by a single individual over its lifetime, assuming that the individual is subject to a particular spatial configuration in the river. This spatial configuration is an asymptotically stable next generation distribution associated with R_0. As a threshold parameter, R_0 is a powerful tool for studying population persistence in demography and ecology. The population will grow if $R_0 > 1$, but the population will become extinct if $R_0 < 1$.

In our benthic-drift model, we assume that individuals do not disperse on the benthos. This results in a system consisting of a reaction-diffusion-advection equation coupled to an ordinary differential equation at every point in space, and hence the solution maps of the system are not compact. Traditional theories of R_0 in infinite-dimensional dynamical systems based on the celebrated Krein–Rutman theorem [9], which was used to analyze model (1.1),

are therefore not applicable to our model. A recent work by Wang and Zhao [31] has developed a theory of R_0 for compartmental epidemic models of reaction-diffusion equations, where some of the diffusion coefficients could be zeros. We adapt this theory to our benthic-drift model and show that it admits a net reproductive rate R_0 that serves as a threshold value for extinction and uniform persistence of the population under investigation.

The paper is organized as follows. In the next section, we introduce a benthic-drift model for a population in a stream. In section 3, we derive three measures of persistence, $R_{\text{loc}}(x)$, $R_\delta(x)$, and R_0 for our model. We show that R_0 can be used to determine the stability of the homogeneous trivial steady state of the model and can therefore be used as a measure of global population persistence. We present numerical methods to calculate R_0 and R_δ. In section 4, we investigate how the water flow, birth rate, transfer rates, and river heterogeneity affect the population persistence by numerically studying the dependence of R_0 and R_δ on these variables. In section 5, we apply R_0 theory to find the critical domain size for the population described by the benthic-drift model. In section 6, we compare the single compartment model (1.1) with the benthic-drift model from the perspectives of theoretical analysis, numerical methods, and biological applications. A discussion section completes the paper.

2. Model. We partition a river into the free-flowing water (or drift zone) and storage zones (or benthic zone) [4, 7]. Assume that the water movement in the storage zone can be neglected. We denote A_d and A_b as the cross-sectional areas of the drift zone and benthic zone, respectively. We consider a population in which individuals live and reproduce in the storage zone, and occasionally enter the water column to drift until they settle in the benthic zone again. Thus, individuals' movement in drifting water can be expressed as a combination of advection (corresponding to the uniform stream flow as experienced by the organisms) and diffusion (corresponding to the heterogeneous stream flow and individual swimming). The mathematical model that describes the spatial dynamics of the population in a stream of longitudinal length L is given by

$$
\begin{cases}
\dfrac{\partial N_d}{\partial t} = \underbrace{\dfrac{A_b(x)}{A_d(x)}\mu(x)N_b}_{\text{transfer from } N_b} - \underbrace{\sigma(x)N_d}_{\text{transfer to } N_b} - \underbrace{m_d(x)N_d}_{\text{mortality}} - \underbrace{\dfrac{Q}{A_d(x)}\dfrac{\partial N_d}{\partial x}}_{\text{advection}} \\
\qquad\qquad + \underbrace{\dfrac{1}{A_d(x)}\dfrac{\partial}{\partial x}\left(D(x)A_d(x)\dfrac{\partial N_d}{\partial x}\right)}_{\text{diffusion}}, \quad x \in (0,L), t > 0, \\
\dfrac{\partial N_b}{\partial t} = \underbrace{f(x,N_b)N_b}_{\text{reproduction}} - \underbrace{m_b(x)N_b}_{\text{mortality}} - \underbrace{\mu(x)N_b}_{\text{transfer to } N_d} + \underbrace{\dfrac{A_d(x)}{A_b(x)}\sigma(x)N_d}_{\text{transfer from } N_d}, \quad x \in (0,L), t > 0, \\
\alpha_1 N_d(0,t) - \beta_1 \dfrac{\partial N_d}{\partial x}(0,t) = 0, \quad t > 0, \\
\alpha_2 N_d(L,t) + \beta_2 \dfrac{\partial N_d}{\partial x}(L,t) = 0, \quad t > 0, \\
N_d(x,0) = N_d^0(x), N_b(x,0) = N_b^0(x), \quad x \in (0,L),
\end{cases}
\tag{2.1}
$$

where $N_d(x,t)$ is the density of individuals at location x in the drift zone at time t, $N_b(x,t)$

is the density of individuals at location x in the benthic zone at time t, μ is the per capital rate at which individuals in the benthic zone enter the drift zone, σ is the per capital rate at which the organisms return to the benthic zone from drifting, $f(x, N_b)$ is the per capita birth rate function, m_b and m_d are mortality rates of benthic individuals and drifting individuals, respectively, $Q > 0$ is the constant stream discharge, $D(x)$ is the spatially variable diffusion coefficient, α_i and β_i are nonnegative constants ($i = 1, 2$), and N_d^0 and N_b^0 are initial distributions of the population in the drifting flow and in the benthos, respectively.

The boundary conditions we could consider are either Dirichlet ($\alpha_i = 1, \beta_i = 0$), Neumann ($\alpha_i = 0,\ \beta_i = 1$), or Robin ($\alpha_i \geq 0, \beta_i \geq 0, \alpha_i + \beta_i \neq 0$) conditions. In particular, we allow for two types of boundary conditions relevant to streams, which we refer to as *hostile* and *Danckwert's* boundary conditions (see, e.g., [22]). Hostile conditions represent zero flux at the stream source (individuals cannot enter or leave the domain at the source) and zero density at the stream outflow (e.g., the stream discharges all individuals into a region such as a salt water, from which they cannot return) [27]:

$$QN_d(0,t) - D(0)A_d(0)\frac{\partial N_d}{\partial x}(0,t) = 0 \quad \text{and} \quad N_d(L,t) = 0. \tag{2.2}$$

Danckwert's conditions also assume zero flux at the stream source, but use a free-flow condition at the stream outflow (individuals leave the domain at the same rate as the advection takes them):

$$QN_d(0,t) - D(0)A_d(0)\frac{\partial N_d}{\partial x}(0,t) = 0 \quad \text{and} \quad \frac{\partial N_d}{\partial x}(L,t) = 0. \tag{2.3}$$

For a derivation and discussion of these boundary conditions from a random-walk perspective, see [20].

In this paper, we make the following assumptions for the functions and parameters in the model (2.1):

(i) $\mu(x)$, $\sigma(x)$, $m_b(x)$, and $m_d(x)$ are nonnegative continuous functions.

(ii) D, A_b, $A_d \in C^2([0, L], (0, \infty))$, and there exist positive constants c_1 and c_2 such that $c_1 < A_d(x), A_b(x) < c_2$ for any $x \in [0, L]$.

(iii) $f : [0, L] \times (0, \infty) \to \mathbb{R}$ is continuous, $f(x, 0) - m_b(x) = \lim_{N_b \to 0^+} f(x, N_b) - m_b(x) < \infty$, $f(x, N_b)$ is monotonically decreasing in N_b, and for each x there exists a unique value $N_b(x) := K(x) > 0$ such that $f(x, K(x)) - m_b(x) = 0$.

We define the strongly elliptic linear operator

$$\mathcal{L} := -\frac{Q}{A_d(x)}\frac{\partial}{\partial x} + \frac{1}{A_d(x)}\frac{\partial}{\partial x}\left(D(x)A_d(x)\frac{\partial}{\partial x}\right), \tag{2.4}$$

which represents both the directed dispersal due to downstream flow and the random dispersal due to turbulence and intrinsic movement of individuals, respectively. Although the operator $\mathcal{L}$ is specific to dispersal in streams, all the results in this paper hold if $\mathcal{L}$ is replaced by a strongly elliptic operator in a general form:

$$\tilde{\mathcal{L}} := -\tilde{a}(x)\frac{\partial}{\partial x} + \tilde{D}(x)\frac{\partial^2}{\partial x^2}. \tag{2.5}$$

The model (2.1) was derived in [20] from a three-dimensional conservation law for movement of individuals in streams. When the parameters A_d, A_b, σ, μ, m_b are constants and $A_d = A_b$, $m_d = 0$, the system (2.1) reduces to the model of [24], which is well understood in the context of critical domain size and propagation speed analysis (further discussion is given in section 5).

3. Theoretical analysis. Our theoretical analysis of population persistence and extinction is based on the following mathematical setting.

In the case where both upstream and downstream boundary value conditions are Neumann or Robin boundary conditions (e.g., Danckwert's boundary conditions), let $X = C([0, L], \mathbb{R})$ denote the Banach space of continuous functions on the interval $[0, L]$ with the supremum norm $\|u\|_\infty = \max_{x\in[0,L]} |u(x)|$ for $u \in X$. The set of nonnegative functions forms a solid cone X_+ in the Banach space X with interior $Int(X_+) = \{u \in X : u > 0, \forall x \in [0, L]\}$. The partial order $\ll$ on X is defined by $u_1 \ll u_2$ provided $u_2 - u_1 \in Int(X_+)$.

In the case where one or two boundary conditions are Dirichlet boundary conditions (e.g., hostile boundary conditions), let $U = C_0([0, L], \mathbb{R})$ denote the Banach space of continuous functions on $[0, L]$ vanishing on the boundary with the cone U_+ of nonnegative functions in U. Let $U_1 = C^1([0, L], \mathbb{R})$ be the Banach space of continuously differentiable functions on [0,L] with the norm $||u||_1 = \max_{x\in[0,L]} |u(x)| + \max_{x\in[0,L]} |u'(x)|$. Let X be the closed subspace of U_1 consisting of continuously differentiable functions vanishing on the boundary. The set $X_+ = X \cap U_+$ is a solid cone in X with nonempty interior in X given by $Int(X_+) = \{u \in X_+ : u(x) > 0$ for all $x \in (0, L), u_x(0) > 0, u_x(L) < 0\}$. We write $u_1 \ll u_2$ if $u_1, u_2 \in X$ and $u_2 - u_1 \in Int(X_+)$, but in this case "$\ll$" does not define a partial order.

By similar arguments to those in [21, Theorem 1 and Remark 1.1] and [12, Lemma 3.1], we have the following result on the well-posedness of the initial boundary value problem (2.1).

Lemma 1. *The system* (2.1) *has a unique solution on* $[0, \infty) \times [0, L]$ *for any initial value in* $X \times X$ *and the solutions to* (2.1) *remain nonnegative if they are nonnegative initially.*

Moreover, we can obtain that (2.1) defines a semiflow $\{\Phi_t\}_{t\geq 0}$ that is continuous from X to X and is strongly order preserving for each $t > 0$ (see also [22, 26]).

3.1. The next generation operator. Note that $(0, 0)$ is the trivial homogeneous steady state of (2.1) and that the associated linearized system of model (2.1) at $(0, 0)$ is

$$
\begin{cases}
\dfrac{\partial N_d}{\partial t} = \dfrac{A_b(x)}{A_d(x)}\mu(x)N_b - \sigma(x)N_d - m_d(x)N_d + \mathcal{L}N_d, \quad x \in (0, L), t > 0,\\
\dfrac{\partial N_b}{\partial t} = f(x, 0)N_b - m_b(x)N_b - \mu(x)N_b + \dfrac{A_d(x)}{A_b(x)}\sigma(x)N_d, \quad x \in (0, L), t > 0,\\
\alpha_1 N_d(0, t) - \beta_1 \dfrac{\partial N_d}{\partial x}(0, t) = 0, \quad t > 0,\\
\alpha_2 N_d(L, t) + \beta_2 \dfrac{\partial N_d}{\partial x}(L, t) = 0, \quad t > 0,\\
N_d(x, 0) = N_d^0(x), \quad N_b(x, 0) = N_b^0(x), \quad x \in (0, L).
\end{cases} \tag{3.1}
$$

Now we define the next generation operator associated with the linearized system (3.1). The operator should map an initial population distribution to its "next generation" distribution

(or its offspring distribution). By studying the properties of the next generation operator, we expect to see whether the population can persist in a stream or not.

Suppose that a population of species is introduced into the stream environment $[0, L]$ with density distribution $(n_d^0, n_b^0) \in X \times X$, and then the individuals of this population experience dispersal in the drift zone and reproduction in the benthic zone until they die. If $(n_d(x,t), n_b(x,t))$ denotes the density of these initial individuals at x at time t, then the population density over time is governed by the model

$$
\begin{cases}
\dfrac{\partial n_d}{\partial t} = \dfrac{A_b(x)}{A_d(x)}\mu(x)n_b - \sigma(x)n_d - m_d(x)n_d + \mathcal{L}n_d, \quad x \in (0,L), t > 0, \\
\dfrac{\partial n_b}{\partial t} = -m_b(x)n_b - \mu(x)n_b + \dfrac{A_d(x)}{A_b(x)}\sigma(x)n_d, \quad x \in (0,L), t > 0, \\
\alpha_1 n_d(0,t) - \beta_1 \dfrac{\partial n_d}{\partial x}(0,t) = 0, \qquad t > 0, \\
\alpha_2 n_d(L,t) + \beta_2 \dfrac{\partial n_d}{\partial x}(L,t) = 0, \qquad t > 0, \\
n_d(x,0) = n_d^0(x), \quad n_b(x,0) = n_b^0(x), \qquad x \in (0,L).
\end{cases} \tag{3.2}
$$

The difference between (3.2) and (3.1) is the lack of reproduction $(f(x,0)N_b))$ in the benthic category. The function $f(x,0)n_b(x,t)$ is the rate of population reproduction by the initial individuals at location x at time t. Therefore, at location x, the total reproduction by initially introduced individuals during their lifetime is given by $\int_0^\infty f(x,0)n_b(x,t)dt$ (or $f(x,0)\int_0^\infty n_b(x,t)dt$), which we call the *next generation distribution* of the initial distribution (n_d^0, n_b^0). Note that we are able to show the existence of $\int_0^\infty n(x,t)dt$ and its continuity with respect to x by explicitly calculating the integral, as shown in (A.20) (see Appendix A.5), and by our model assumptions. This leads us to the following definition.

Definition 2. *The next generation operator* $\Gamma : X \times X \to X \times X$ *associated with* (3.1) *is defined as*

$$
\Gamma \begin{pmatrix} n_d^0 \\ n_b^0 \end{pmatrix}(x) := \int_0^\infty \begin{pmatrix} 0 & 0 \\ 0 & f(x,0) \end{pmatrix} \begin{pmatrix} n_d(x,t) \\ n_b(x,t) \end{pmatrix} dt = \begin{pmatrix} 0 \\ f(x,0)\displaystyle\int_0^\infty n_b(x,t)dt \end{pmatrix}, \tag{3.3}
$$

where $(n_d(x,t), n_b(x,t))$*, the distribution of the initially introduced individuals at time* t*, is the solution of* (3.2).

3.2. Three measures of population persistence. Recently, [19] proposed three relevant measures of population persistence that relate to lifetime reproductive output, survival, and dispersal in a spatially variable environment. These measures, described in the introduction, were applied in [22] to analyze an advection-diffusion-reaction model for populations in streams, where the whole river channel was regarded as a drift zone. Here we adapt these measures to provide a new way of analyzing the benthic-drift model (2.1).

In this paper, we say that a population described by (2.1) will persist if there exists $\epsilon > 0$ such that

$$
\limsup_{t\to\infty} ||(N_d, N_b) - (0,0)||_\infty = \limsup_{t\to\infty} \max_{x\in[0,L]} \{N_d(t,x), N_b(t,x)\} \geq \epsilon. \tag{3.4}
$$

Otherwise, we say that the population will be washed out. In particular, the population will be washed out if the trivial steady state $(N_d^*, N_b^*) = (0, 0)$ of (2.1) is stable in the sense that it attracts all solutions with small initial values.

Now we define three measures of population persistence for model (2.1).

Measure 1: Fundamental niche, $R_{\mathbf{loc}}(x)$. The first measure of local persistence, denoted by $R_{\mathrm{loc}}(x)$, determines the fundamental niche of the species. Recall that the fundamental niche of an organism in its ecosystem is the full range of environmental conditions and resources (biological and physical) that the organism can possibly occupy and use, especially when limiting factors are absent. We assume that the individual only experiences birth and death after being introduced into the stream but excludes dispersal processes during its lifetime. In this case, (3.1) reduces to

$$\begin{cases} \dfrac{dN_b}{dt} = f(x,0)N_b - m_b(x)N_b, & x \in (0,L), t > 0, \\ N_b(x,0) = N_b^0(x), & x \in (0,L). \end{cases} \tag{3.5}$$

We define $R_{\mathrm{loc}}(x)$ as the the number of offspring produced by an individual introduced at $x \in [0, L]$ in the benthic zone over its lifetime. That is,

$$R_{\mathrm{loc}}(x) = f(x,0)\int_0^\infty n_b(x,t)dt, \tag{3.6}$$

where $n_b(x,t)$ is the solution to the initial-value problem

$$\begin{cases} \dfrac{dn_b}{dt} = -m_b(x)n_b, & x \in (0,L), t > 0, \\ n_b(x,0) = 1, & x \in (0,L). \end{cases} \tag{3.7}$$

Solving (3.7) yields $n_b(x,t) = e^{-m_b(x)t}dt$ and therefore

$$R_{\mathrm{loc}}(x) = f(x,0)\int_0^\infty e^{-m_b(x)t}dt = \frac{f(x,0)}{m_b(x)}, \tag{3.8}$$

which is the per capital reproduction rate times the average life span of an individual at x. Thus, $R_{\mathrm{loc}}(x) > 1$ is equivalent to $f(x,0) > m_b(x)$, i.e., the per capital reproduction rate is greater than mortality rate; $R_{\mathrm{loc}}(x) < 1$ is equivalent to $f(x,0) < m_b(x)$. It follows from the definition of $R_{loc}(x)$ that if $R_{\mathrm{loc}}(x) > 1$, an individual introduced at x will produce more than one offspring at x in the next generation and the population size at x will increase over the generations. Therefore, locations with $R_{\mathrm{loc}}(x) > 1$ correspond to the fundamental niche of the species.

Measure 2: Source-sink distribution, $R_\delta(x)$. The second measure of local persistence, denoted $R_\delta(x)$, describes the number of offspring produced by an individual introduced at x in the benthic zone and undergoing birth, death, and dispersal dynamics. It determines the *source-sink distribution* in the stream. To define $R_\delta(x)$, we return to the full spatial model (3.1). The distribution of offspring, produced by a single individual introduced at x in the benthic zone, is given by

$$f(z,0)\int_0^\infty n_b(z,t)dt, \tag{3.9}$$

where $n_b(z,t)$ is the second compartment of the solution of (3.2) (replacing spatial variable x by z) with initial distribution $(n_d(z,0), n_b(z,0)) = (0, \delta(z-x))$ and $\delta(\cdot)$ is the Dirac delta function.

We then define $R_\delta(x)$ as

$$R_\delta(x) = \int_0^L f(z,0) \int_0^\infty n_b(z,t)dtdz. \tag{3.10}$$

Locations where $R_\delta(x) > 1$ act as sources, because an individual introduced at location x will produce more than one offspring in the whole stream domain $[0, L]$. Locations where $R_\delta(x) < 1$ serve as sinks, because the lifetime reproductive output of an individual introduced at location x will results in less than one offspring in the whole stream. Thus, $R_\delta(x)$ is a measure of the source-sink dynamics in the stream.

Measure 3: Net reproductive rate, R_0. This measure is defined for the population's global persistence. For any initial distribution $(N_d^0(x), N_b^0(x))$ of the spatial model (3.1), the associated next generation distribution is

$$\Gamma \begin{pmatrix} N_d^0 \\ N_b^0 \end{pmatrix}(x) = \begin{pmatrix} 0 \\ f(x,0) \int_0^\infty n_b(x,t)dt \end{pmatrix}, \tag{3.11}$$

where $n_b(x,t)$ solves (3.2) with initial condition (N_d^0, N_b^0). Define

$$R_0 := r(\Gamma), \tag{3.12}$$

where $r(\Gamma)$ is the spectral radius (see, e.g., [8]) of the linear operator Γ on $X \times X$. We call R_0 the *net reproductive rate*. R_0 represents the average number of offspring an individual may produce during its lifetime.

3.3. Persistence theory. In this subsesction, we will show that R_0 can predict global persistence or extinction of the focal population.

First, we consider an eigenvalue problem. Substituting $N_d(x,t) = e^{\lambda t}\phi_1(x)$ and $N_b(x,t) = e^{\lambda t}\phi_2(x)$ into (3.1), we obtain the associated elliptic eigenvalue problem

$$\begin{cases} \dfrac{A_b(x)}{A_d(x)}\mu(x)\phi_2 - \sigma(x)\phi_1 - m_d(x)\phi_1 + \mathcal{L}\phi_1 = \lambda\phi_1, \quad x \in (0,L), \\ f(x,0)\phi_2 - m_b(x)\phi_2 - \mu(x)\phi_2 + \dfrac{A_d(x)}{A_b(x)}\sigma(x)\phi_1 = \lambda\phi_2, \quad x \in (0,L), \\ \alpha_1\phi_2(0) - \beta_1 \dfrac{d\phi_2}{dx} \mid_{x=0} = 0, \\ \alpha_2\phi_2(L) + \beta_2 \dfrac{d\phi_2}{dx} \mid_{x=L} = 0. \end{cases} \tag{3.13}$$

The following result follows from similar arguments as in Lemma 4.1 in [31]. The proof is given in Appendix A.1.

Theorem 3. *Problem* (3.13) *has a simple principal eigenvalue* λ^* *with a positive eigenfunction.*

By the results in Theorem 3.1(i) and Remark 3.1 in [31], we have the following result that relates R_0 to the principal eigenvalue λ^* of (3.13).

Lemma 4. *$R_0 - 1$ has the same sign as λ^*, where λ^* is the principal eigenvalue of* (3.13).

The following result implies that R_0 is a threshold value for the stability of the trivial homogeneous steady state solution $(N_d^*, N_b^*) \equiv (0,0)$ of the nonlinear population model (2.1). Hence, the threshold $R_0 = 1$ separates population extinction from population persistence for the nonlinear model (2.1). The proof of Theorem 5 is provided in Appendix A.2.

Theorem 5.

(i) *If $R_0 < 1$, then $(0,0)$ is asymptotically stable for model* (2.1).

(ii) *If $R_0 > 1$, then $(0,0)$ is unstable for model* (2.1) *and the population persists according to definition* (3.4).

3.4. Computation of R_0 and R_δ. The next generation operator Γ is defined in (3.3) in terms of an auxiliary time-dependent problem (3.2). Here we will find another spatial operator $\hat{\Gamma}$, which is not related to a time-dependent problem but shares the same spectral radius with Γ. We also obtain an alternative formula for $R_\delta(x)$ by investigating the dynamics of (3.2). We then provide numerical methods for calculating R_0 and $R_\delta(x)$.

3.4.1. Operator $\hat{\Gamma}$ and R_0. We define $\hat{\Gamma} : X \to X$ as

(3.14)
$$\hat{\Gamma}(\varphi)(x) := \frac{f(x,0)\varphi(x)}{m_b(x)+\mu(x)} + \frac{\sigma(x)A_d(x)}{(m_b(x)+\mu(x))A_b(x)} \int_0^L k(x,y) \frac{f(y,0)\mu(y)A_b(y)\varphi(y)}{(m_b(y)+\mu(y))A_d(y)} dy \quad \forall \varphi \in X,$$

where $k(x,y)$ is the solution of the ordinary boundary value problem

(3.15)
$$\begin{cases} \left(\mathcal{L} - \sigma(x) - m_d(x) + \dfrac{\sigma(x)\mu(x)}{m_b(x)+\mu(x)}\right) k(x,y) = -\delta(x-y), & x \in (0,L), \\ \alpha_1 k(0,y) - \beta_1 k'(0,y) = 0, \\ \alpha_2 k(L,y) + \beta_2 k'(L,y) = 0 \end{cases}$$

for a fixed value of $y \in (0,L)$ (here $'$ denotes differentiation with respect to x). Note that the solution to (3.15) is a Green's function (see (2-11) in Chapter 7 in [10], (2.9) in Chapter 3 in [28], or Appendix B in [22]). It is worthwhile to point out that $\hat{\Gamma}(\varphi)(x)$ represents the offspring distribution of the initial population $\varphi(x)$ only distributed on the benthos. Then we can obtain the following result with the proof given in Appendix A.3.

Theorem 6. *The spectral radius of Γ is the same as the spectral radius of $\hat{\Gamma}$, i.e., $r(\Gamma) = r(\hat{\Gamma})$.*

Thus, $R_0 = r(\hat{\Gamma})$ and it suffices to calculate the spectral radius of $\hat{\Gamma}$ to determine population persistence or extinction for model (2.1).

When the coefficients describing birth ($f(x,0)$), mortality ($m_b(x)$ and $m_d(x)$), transfer ($\sigma(x)$ and $\mu(x)$), and cross-sectional areas ($A_b(x)$ and $A_d(x)$) are spatially homogeneous, we show in the following corollary that R_0 is the principal eigenvalue of $\hat{\Gamma}$. See Appendix A.4 for the proof.

Corollary 7. *Assume that $f(x,0) \equiv f$, $m_b(x) \equiv m_b$, $m_d(x) \equiv m_d$, $\sigma(x) \equiv \sigma$, $\mu(x) \equiv \mu$, $A_b(x) \equiv A_b$, and $A_d(x) \equiv A_d$. Then R_0 is the principal eigenvalue of $\hat{\Gamma}$ with a positive*

eigenfunction and

$$R_0 = \frac{f}{m_b + \mu} + \frac{f\sigma\mu}{(m_b + \mu)^2}\varsigma^*, \tag{3.16}$$

where ς^* *is the principal eigenvalue of* Φ*, defined as*

$$\Phi(\varphi)(x) := \int_0^L k(x, y)\varphi(y)dy, \ \forall \varphi \in X, \tag{3.17}$$

where $k(x, y)$ *satisfies* (3.15).

3.4.2. An alternative formula for $R_\delta(x)$. The following proposition gives an alternative formula to calculate the source-sink distribution $R_\delta(x)$. The proof can be found in Appendix A.5.

Proposition 8. *The source-sink distribution,* $R_\delta(x)$*, defined in* (3.10)*, can be calculated by the following formula:*

(3.18)
$$R_\delta(x) = \frac{f(x, 0)}{m_b(x) + \mu(x)} + \frac{\mu(x)A_b(x)}{(m_b(x) + \mu(x))A_d(x)} \int_0^L f(z, 0)k(z, x)\frac{\sigma(z)A_d(z)}{(m_b(z) + \mu(z))A_b(z)}dz$$

for any $x \in (0, L)$*, where* k *is defined by* (3.15).

3.4.3. Numerical methods. In what follows, we present numerical methods to calculate R_0 and R_δ.

From the definition of R_0 in (3.12) and Theorem 6, we have

$$R_0 = r(\Gamma) = r(\hat{\Gamma}) = \sup\{|\lambda|, \ \lambda \in \sigma(\hat{\Gamma})\}, \tag{3.19}$$

where $\hat{\Gamma}$ is defined in (3.14), $\sigma(\hat{\Gamma}) = \{\lambda \in \mathbb{C}, \ \lambda I - \hat{\Gamma}$ is not invertible$\}$, and I is an identity operator. For most cases it is not possible to find an analytic expression of the spectral radius of an operator. One of the principal projection methods, the collocation method, reviewed in ([6], section 3.1.1) and restated in [22], provides a practical approach for approximating an operator. Here we apply such a method to numerically approximate $\hat{\Gamma}$ on X and then approximate the spectral radius of $\hat{\Gamma}$.

We divide the interval $[0, L]$ into $n - 1$ equal subintervals $[x_j, x_{j+1}]$, $j = 1, 2, \ldots, n - 1$, where $0 = x_1 < x_2 < \cdots < x_n = L$. Denote the size of subintervals by Δx. For any $\varphi \in X$, we consider its piecewise linear approximation by

$$\varphi(x) \approx \sum_{j=1}^{n} \varphi(x_j)e_j(x), \tag{3.20}$$

where $e_j(x), j = 1, 2, \ldots, n$, piecewise linear basis "hat" functions, depicted in Figure 1, are defined by

$$e_j(x) = \max\left\{0, 1 - \frac{|x - x_j|}{\Delta x}\right\}, \qquad x \in [0, L], \quad j = 1, 2, \ldots, n. \tag{3.21}$$

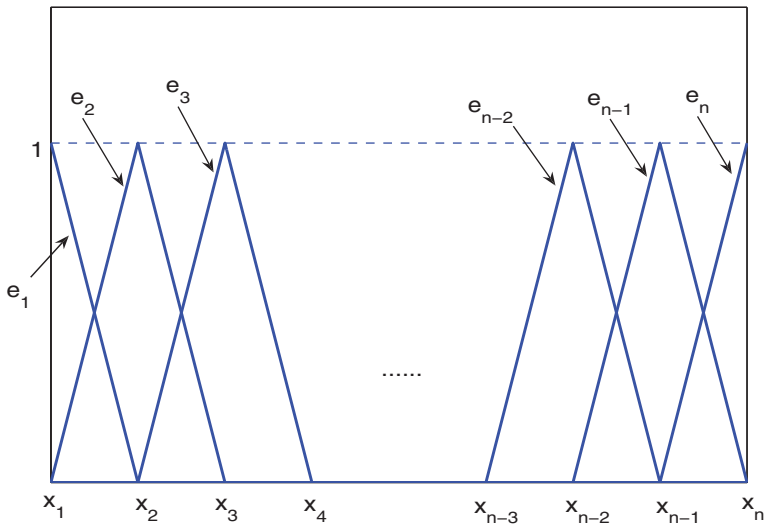

Figure 1. *Hat functions.*

Let $X_n = \text{span}\{e_1, e_2, \ldots, e_n\}$, then the Banach space X (see section 3 for definition) can be approximated by $\{X_n\}_{n=1}^{\infty}$, a sequence of finite-dimensional subspaces of X.

Plugging (3.20), the basis function representation of $\varphi(x)$, into (3.14), we have

$$
\begin{aligned}
(\hat{\Gamma}\varphi)(x) \approx & \frac{f(x,0)}{m_b(x)+\mu(x)} \sum_{j=1}^{n} \varphi(x_j) e_j(x) \\
& + \frac{\sigma(x) A_d(x)}{(m_b(x)+\mu(x)) A_b(x)} \int_0^L k(x,y) \frac{f(y,0)\mu(y) A_b(y)}{(m_b(y)+\mu(y)) A_d(y)} \sum_{j=1}^{n} \varphi(x_j) e_j(y) dy.
\end{aligned} \tag{3.22}
$$

By exploiting the specific basis functions, we find

$$
\begin{aligned}
& \int_0^L k(x,y) \frac{\mu(y) A_b(y)}{(m_b(y)+\mu(y)) A_d(y)} \sum_{j=1}^{n} \varphi(x_j) e_j(y) dy \\
& = \varphi(x_1) \int_{x_1}^{x_2} k(x,y) \frac{\mu(y) A_b(y)}{(m_b(y)+\mu(y)) A_d(y)} e_1(y) dy \\
& \quad + \sum_{j=2}^{n-1} \varphi(x_j) \int_{x_{j-1}}^{x_{j+1}} k(x,y) \frac{\mu(y) A_b(y)}{(m_b(y)+\mu(y)) A_d(y)} e_j(y) dy \\
& \quad + \varphi(x_n) \int_{x_{n-1}}^{x_n} k(x,y) \frac{\mu(y) A_b(y)}{(m_b(y)+\mu(y)) A_d(y)} e_n(y) dy.
\end{aligned} \tag{3.23}
$$

Applying collocation points x_i, $i = 1, 2, \ldots, n$, to (3.22) and (3.23), we approximate the

operation (3.14) by the operation of a large matrix, that is,

$$\hat{\Gamma}(\varphi)\begin{pmatrix} x_1 \\ x_2 \\ \cdots \\ x_n \end{pmatrix} \approx \hat{\Gamma}_n \begin{pmatrix} \varphi(x_1) \\ \varphi(x_2) \\ \cdots \\ \varphi(x_n) \end{pmatrix} \quad \forall \varphi \in X, \tag{3.24}$$

where $\hat{\Gamma}_n = \hat{\Gamma}_n^{(1)} + \hat{\Gamma}_n^{(2)}$, with

$$\hat{\Gamma}_n^{(1)} = \operatorname{diag}\left(\frac{f(x_1,0)}{m_b(x_1)+\mu(x_1)}, \ldots, \frac{f(x_n,0)}{m_b(x_n)+\mu(x_n)}\right), \tag{3.25}$$

and $\hat{\Gamma}_n^{(2)}$, an n by n matrix with entries

(3.26)

$$(\hat{\Gamma}_n)_{i,1} = \frac{\sigma(x_i)A_d(x_i)}{(m_b(x_i)+\mu(x_i))A_b(x_i)} \int_{x_1}^{x_2} k(x_i,y) \frac{f(y,0)\mu(y)A_b(y)}{(m_b(y)+\mu(y))A_d(y)} e_1(y)dy, \quad i = 1, \ldots, n,$$

$$(\hat{\Gamma}_n)_{i,j} = \frac{\sigma(x_i)A_d(x_i)}{(m_b(x_i)+\mu(x_i))A_b(x_i)} \int_{x_{j-1}}^{x_{j+1}} k(x_i,y) \frac{f(y,0)\mu(y)A_b(y)}{(m_b(y)+\mu(y))A_d(y)} e_j(y)dy,$$
$$i = 1, \ldots, n, j = 2, \ldots, n-1,$$

$$(\hat{\Gamma}_n)_{i,n} = \frac{\sigma(x_i)A_d(x_i)}{(m_b(x_i)+\mu(x_i))A_b(x_i)} \int_{x_{n-1}}^{x_n} k(x_i,y) \frac{f(y,0)\mu(y)A_b(y)}{(m_b(y)+\mu(y))A_d(y)} e_n(y)dy, \quad i = 1, \ldots, n.$$

Now we use the matrix operator $\hat{\Gamma}_n$ to approximate $\hat{\Gamma}$. Thus, R_0, the spectral radius of the operator $\hat{\Gamma}$, can be approximated by the spectral radius of the matrix $\hat{\Gamma}_n$, for very large n.

We observe that all elements of the matrix $\hat{\Gamma}_n$, determined by population vital rates and transfer rates, are nonnegative. Thus, the Perron–Frobenius theorem implies the following results: (1) $\hat{\Gamma}_n$ has a positive real eigenvalue $\lambda_{1,n}$, called the Perron–Frobenius eigenvalue or the principal eigenvalue, such that any other eigenvalue (possibly, complex) is strictly smaller than $\lambda_{1,n}$ in absolute value. That is, the spectral radius of matrix $\hat{\Gamma}_n$ is equal to $\lambda_{1,n}$. (2) There exists an eigenvector $[\varphi(x_1), \ldots, \varphi(x_n)]^T$ of $\hat{\Gamma}_n$ associated with eigenvalue $\lambda_{1,n}$ such that all components of this eigenvector are positive.

Based on the above results, we approximate R_0 by the principal eigenvalue $\lambda_{1,n}$ of $\hat{\Gamma}_n$. Applying the hat functions (3.21) to the eigenvector $[\varphi(x_1), \ldots, \varphi(x_n)]^T$ yields a function

$$\sum_{j=1}^{n} \varphi(x_j) e_j(x) := \phi(x). \tag{3.27}$$

We notice that ϕ is an approximation of the stable next generation distribution; that is, if the current population distribution is given by $\phi(x)$, then its offspring distribution can be approximated by $R_0\phi(x)$, provided that we use $\hat{\Gamma}_n$ to approximate $\hat{\Gamma}$. For brevity we henceforth refer to ϕ as the *next generation function*.

When the coefficients describing birth ($f(x,0)$), mortality ($m_b(x)$ and $m_d(x)$), transfer ($\sigma(x)$ and $\mu(x)$), and cross-sectional areas ($A_b(x)$ and $A_d(x)$) are spatially homogeneous, the matrix $\hat{\Gamma}_n$ can be simplified and we can use the same method to approximate R_0.

Moreover, by the meaning of R_δ, we can approximate $R_\delta(x)$ by

$$R_\delta(x) = \sum_{j=1}^{n} R_\delta(x_j) e_j(x), \tag{3.28}$$

where $R_\delta(x_j)$ is defined by (3.18).

4. Numerical results. In this section, we study how the net reproductive rate, stream flow, transfer rates, and river heterogeneity affect the population persistence through numerical simulations. Consider model (3.1) with hostile boundary conditions (2.2). We assume A_d, m_d, m_b, D, μ, and σ in (3.1) are constants but allow the birth rate f and the size of the benthic zone A_b to vary in space. Following [22], we choose f to be a linearly increasing function with distance downstream,

$$f(x) = f_{\min} + \frac{x}{L}(f_{\max} - f_{\min}), \quad x \in [0, L], \tag{4.1}$$

where $f_{\min}$ and $f_{\max}$ are the birth rates at the upstream and downstream boundaries of the stream, respectively, with $0 \le f_{\min} \le f_{\max}$. Set $v = Q/A_d$. Then (3.1) reduces to the following benthic-drift model:

$$\begin{cases} \dfrac{\partial N_d}{\partial t} = \dfrac{\mu A_b(x)}{A_d} N_b - (\sigma + m_d) N_d - v\dfrac{\partial N_d}{\partial x} + D\dfrac{\partial^2 N_d}{\partial x^2}, & x \in (0, L), t > 0, \\ \dfrac{\partial N_b}{\partial t} = (f(x,0) - m_b - \mu) N_b + \dfrac{\sigma A_d}{A_b(x)} N_d, & x \in (0, L), t > 0, \\ v N_d(0,t) - D\dfrac{\partial N_d}{\partial x}(0,t) = 0, \quad N_d(L,t) = 0, & t > 0, \\ N_d(x,0) = N_d^0(x), \quad N_b(x,0) = N_b^0(x), & x \in (0, L). \end{cases} \tag{4.2}$$

4.1. The action of the next generation operator. We begin by studying the relationship between the long-term behavior of the population model (4.2) and the next generation operator. To this end, we numerically solve the population model (top row of Figure 2). To show the action of the next generation operator, we also numerically approximate R_0 and its associated next generation function $\phi(x)$ (see (3.27)) (bottom row of Figure 2) using the collocation method presented in section 3.4. As we see from Figure 2, the value of the net reproductive rate R_0 determines the eventual fate of the population, persistence ($R_0 > 1$) or washout ($R_0 < 1$).

4.2. The effect of the flow velocity, birth rate, and settling rate on R_δ and R_0. We then consider the source-sink regions in the stream by computing $R_\delta(x)$. We compare $R_\delta(x)$ in the case where the birth rate varies spatially to the case where the birth rate is the constant average $f = (f_{\min} + f_{\max})/2$. The results are presented in Figure 3 for three different settling rates and two different stream flows. The dispersal, described by Green's functions $k(x, y)$, is also shown for low and high flows (middle column of Figure 3). An analytic expression for the Green's function $k(x, y)$ can be obtained based on (3.15) when the involved parameters are constants (see Appendix B in [22]). Comparing the solid, dashed, and dotted lines for each case in Figure 3, we see that different settling rates lead to different source-sink regions

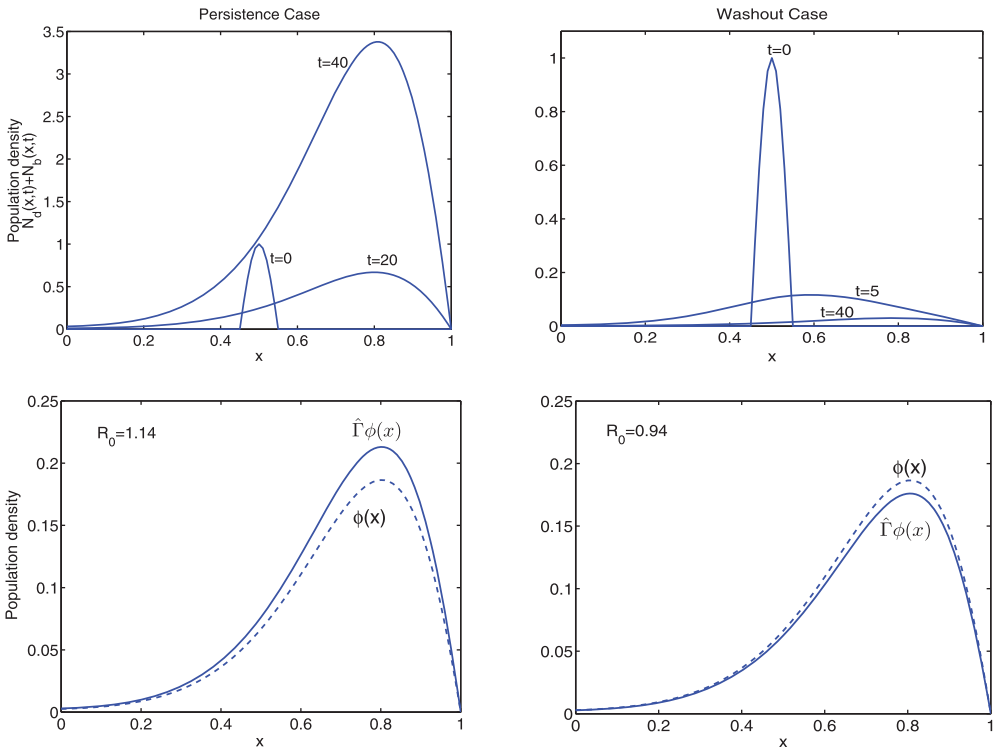

Figure 2. *The long-term population persistence is determined by the action of the next generation operator on the next generation function ϕ. R_0, $\phi(x)$, and $\hat{\Gamma}\phi(x)$ are computed using the numerical method developed in section 3.4.3. The birth rate function $f(x)$ is given by (4.1) with $f_{\min} = 0.4$ and $f_{\max} = 1.2$. Other parameters: $L = 1$, $m_d = m_b = 0.4$, $D = 0.01$, $v = 0.03$, $A_d = A_b$, $\mu = 2$. Depending on the settling rate σ, the population either persists (left column: $\sigma = 2.2$) or is washed out (right column: $\sigma = 1.4$) over time.*

and different dispersal kernels. More precisely, $R_\delta(x)$ increases with increasing settling rate, which results in increased source regions (where $R_\delta(x) > 1$) and decreased sink regions (where $R_\delta(x) < 1$). Also, an increased settling rate leads to decreased dispersal.

When the birth rate is constant in space (left column of Figure 3), the flow can result in the appearance of a sink region associated with the downstream boundary conditions. As the flow increases, the size of the sink region increases. This is because individuals are washed out more quickly with increasing flow and hence are unable to contribute enough offspring to the next generation. In the case where the birth rate is variable in space (right column of Figure 3), new upstream sink regions appear even when the flow is low (right top panel of Figure 3). As the flow increases, the middle parts of the stream are source regions and the upstream and the downstream become sink regions (right bottom panel of Figure 3). Increasing flow causes the size of source regions to become smaller and the size of sink regions to become larger. This is because when downstream birth rates are higher than upstream birth rates, increased flow plays a trade-off role. The flow will transport individuals from upstream to downstream locations where the population has a higher birth rate. Therefore, individuals that are transported into a better habitat in the downstream are able to contribute more offspring to the next generation during their lifetime. However, increased flow also causes loss

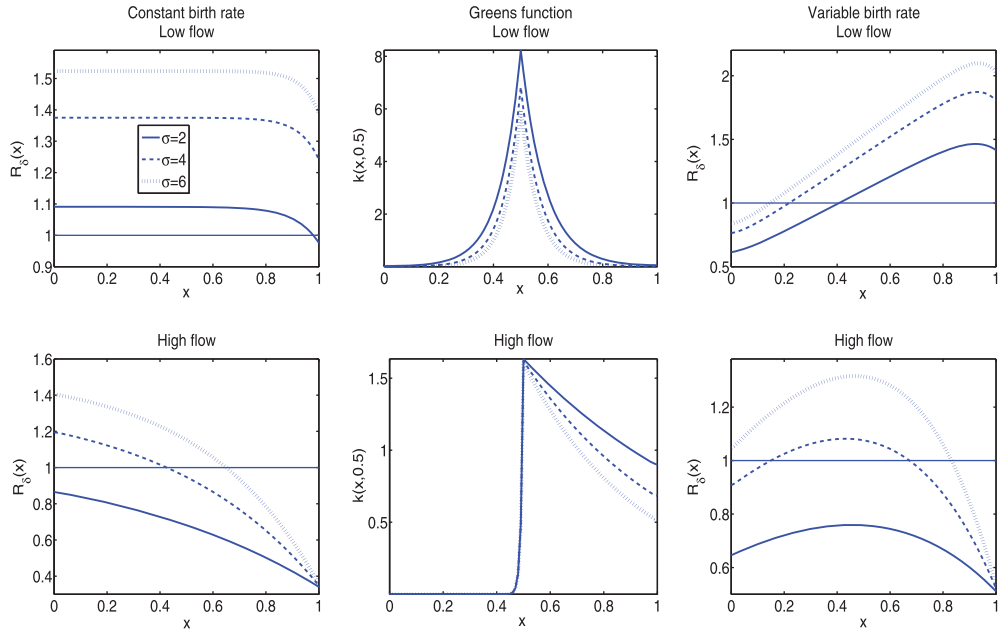

Figure 3. *$R_\delta(x)$ for several flow speeds and settlement rates. Left column: birth rate f is constant ($f = 0.8$). Right column: birth rate $f(x)$ increases linearly with distance downstream, given by (4.1) with $f_{\min} = 0.4$ and $f_{\max} = 1.2$. In each case, Green's functions are shown in the middle column. $D = 0.005$, other parameters are the same as those in Figure 2.*

and possible washout as individuals exit through the downstream boundary. These contrasting effects yield the trade-off for increased flow.

To understand how flow and settling rates interact to influence the source-sink regions and R_0, again we consider a stream where population has a constant birth rate in space (left panel of Figure 4) and a stream where population has a variable birth rate in space (right panel of Figure 4). We plot the proportion of habitat where $R_\delta(x) > 1$ as a function of flow speed and settling rate for each stream (contour lines in Figure 4). For the same range of flow speeds and settling rates, we also calculate R_0 and shade the regions in which $R_0 > 1$ in the σv-plane.

When the birth rate is constant, the effect of the interaction between flow and settling rate on the size of the source region is evident over a range of values (left panel of Figure 4). The maximum size of the source region appears when the flow is low and the settling rate is high. However, when the birth rate is spatially variable, as shown by the right panel of Figure 4, the source region reaches a maximum size when the flow is medium and the settling rate is high. The medium flow is able to carry sufficient individuals to downstream where they have higher birth rate.

As shown in Figure 4, the maximum flow speed permitting persistence ($R_0 > 1$) increases from the left panel (spatially constant birth rate) to the right panel (linearly increasing birth rate). This indicates that high birth rate near the downstream boundary permits persistence under increased stream flow as compared to the constant environment case.

Comparing the results for R_δ with those for R_0 shown by Figure 4, we see that it is possible to have $R_0 < 1$ even when the proportion of the domain where $R_\delta(x) > 1$ is large (say greater

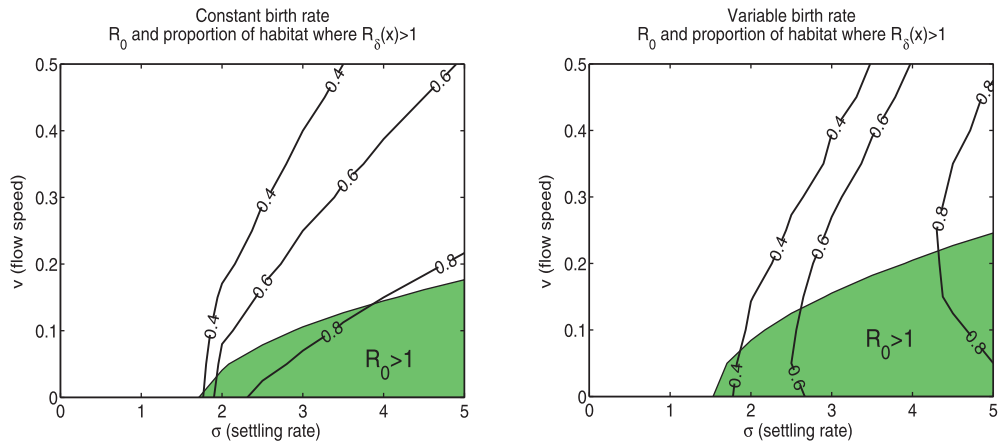

Figure 4. *The proportion of habitat where $R_\delta(x) > 1$ for a range of flow speeds and settling rates. Left column: the birth rate f is constant ($f = 0.8$). Right column: the birth rate function $f(x)$ is given by (4.1) with $f_{\min} = 0.4$ and $f_{\max} = 1.2$. The curves represent the proportions 0.4, 0.6, and 0.8, respectively. The corresponding regions in which $R_0 > 1$ are shown by shading. The parameters other than v and σ are the same as those in Figure 2.*

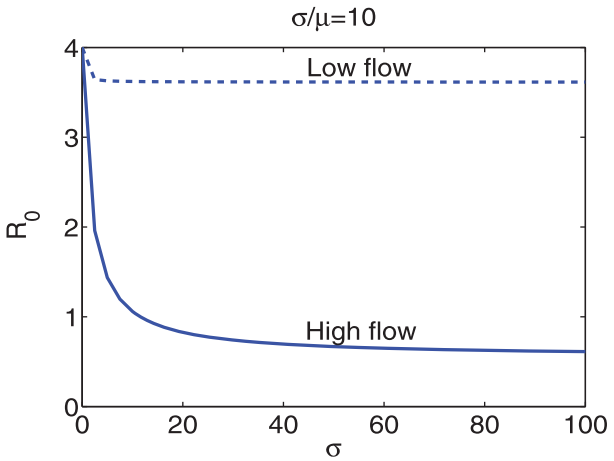

Figure 5. *Dependence of R_0 on transfer rates. The birth rate $f = 0.8$ is constant ($f = 0.8$), $m_d = 0.2, m_b = 0.2, D = 0.005$, $A_d = A_b$.*

than 0.5), and it is possible to have $R_0 > 1$ even when the proportion of the domain where $R_\delta(x) > 1$ is small (say less that 0.5). In other words, population might be washed out even if the majority of the domain are sources, and population might be able to persist even if the majority of the domain are sinks. Therefore, the size of the source region cannot be used to determine the global persistence or extinction for populations in streams.

4.3. The dependence of R_0 on transfer rates. To see how transfer rates affect the population persistence, we obtain R_0 as a function of $\sigma \in [0, 100]$ for a fixed ratio $\sigma/\mu = 10$ in Figure 5. We expect σ/μ to be large because little time is spent in flow relative to benthos. The numerical results show that R_0 decreases as the transfer rate increases and R_0 reaches a

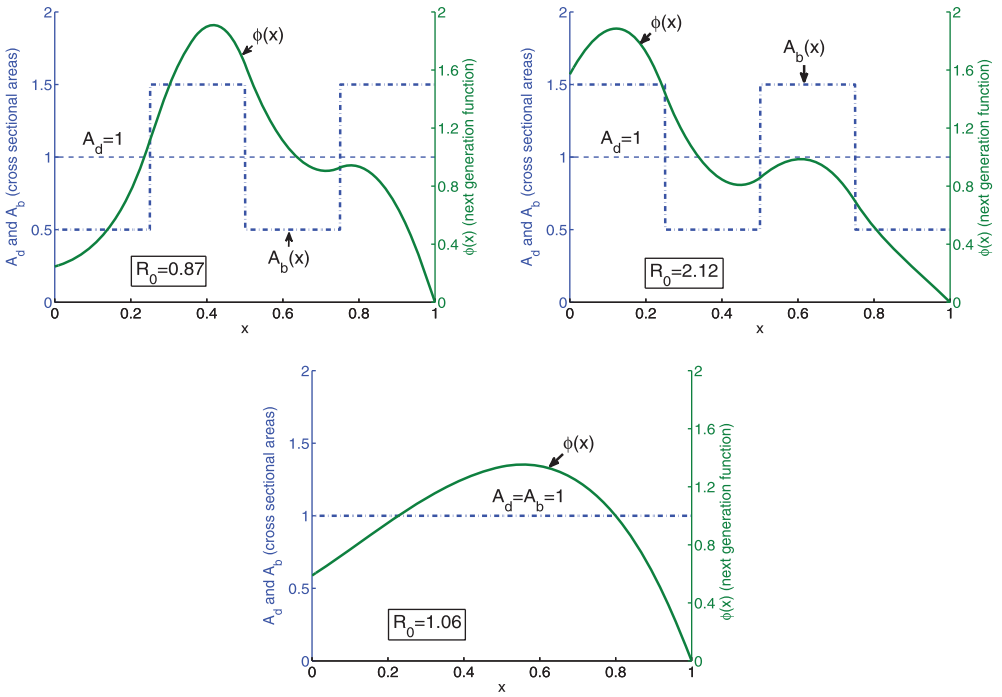

Figure 6. *The net reproductive rate R_0 and corresponding normalized next generation function for several different rivers. $A_b = 0.5$ represents shallows and $A_b = 1.5$ denotes deep pools. $L = 1$, $f = 0.8$, $\sigma = 2.2$. Other parameters are the same as those in Figure 2.*

stable minimum value as the transfer rate increases further. Note that, when the transfer rates are very large, the individuals move very frequently between the drift zone and the benthic zone. In this case, the whole stream becomes more like just one zone and the benefit of the benthic zone becomes less significant. In this sense, Figure 5 also indicates that the benthic component positively affects the ability of the population to resist being washed out.

4.4. The effect of river heterogeneity on R_0. Deep pools and shallows in a river are examples of heterogeneities that typically occur on shorter spatial scales than the entire stretch of a river. To investigate how the heterogeneous landscapes affect the persistence of a population in a river, we consider a spatially periodic pool-shallow river. Assume that the cross-sectional area of the drift zone A_d is a constant, and that the cross-sectional area of the benthic zone varies periodically. We choose $A_d = 1$ and $A_b(x)$ to be a periodic piecewise constant function in which $A_b = 0.5$ represents shallows and $A_b = 1.5$ represents deep pools (Figure 6). We compare the net reproductive rate R_0 and corresponding normalized next generation function $\phi(x)$ (with $\int_0^1 \phi(x)dx = 1$) for populations living in different rivers. The first row of Figure 6 shows that the population has a lower R_0 when there is a shallow in the upstream and a pool in the downstream (left panel of the top row), and the population has a higher R_0 when there is a pool in the upstream and a shallow in the downstream (right panel of the top row).

Individuals grow and reproduce in benthic zones. The deeper the benthic zone is, the easier it is for them to grow. Note that the next generation function $\phi(x)$ associated with R_0

describes the stable next generation population distribution in a river. Figure 6 indicates that when deep pools are close to the upstream, more offspring are produced and live upstream. However, when deep pools are located downstream, more offspring are produced and live downstream where they might easily be washed out.

5. An application of R_0 theory: Finding the critical domain size. In this section, we show that the critical domain size L_{crit} (i.e., the minimal length for a population to persist in a river) can be found by using the net reproductive rate R_0.

Consider the special case of (3.1), where $m_d, m_b, f, \mu, \sigma, D$, and $A_d = A_b$ are constants. Let $v = Q/A_d$, then model (3.1) reduces to the following system:

$$
\begin{cases}
\dfrac{\partial N_d}{\partial t} = -m_d N_d + \mu N_b - \sigma N_d - v\dfrac{\partial N_d}{\partial x} + D\dfrac{\partial^2 N_d}{\partial x^2}, \quad x \in (0, L), t > 0, \\
\dfrac{\partial N_b}{\partial t} = f N_b - m_b N_b - \mu N_b + \sigma N_d, \quad x \in (0, L), t > 0, \\
\alpha_1 N_d(0,t) - \beta_1 \dfrac{\partial N_d}{\partial x}(0,t) = 0, \quad t > 0, \\
\alpha_2 N_d(L,t) + \beta_2 \dfrac{\partial N_d}{\partial x}(L,t) = 0, \quad t > 0, \\
N_d(x,0) = N_d^0(x), \quad N_b(x,0) = N_b^0(x), \quad x \in (0, L).
\end{cases} \tag{5.1}
$$

In the case where $m_d = 0$ (i.e., the mortality rate of the population in the drifting flow was ignored), the critical domain size for (5.1) under hostile boundary conditions (2.2) was shown in [24]. If $f > m_b + \mu$, persistence is guaranteed, irrespective of the domain length and the advection speed. If $f \le m_b + \mu$ and $v < 2\sqrt{D[\sigma\mu/(m_b + \mu - f) - \sigma]} := c^*$, then the critical domain size is given by

$$
L_{\text{crit}} = \frac{2D}{\sqrt{4D\left(\frac{\sigma\mu}{m_b+\mu-f} - \sigma\right) - v^2}} \left(\pi - \arctan\left(\sqrt{\frac{4D}{v^2}\left(\frac{\sigma\mu}{m_b + \mu - f} - \sigma\right) - 1}\right)\right). \tag{5.2}
$$

Note that the original expression for the critical domain size L_{crit} in [24] should be adjusted to (5.2) in terms of the sign of the involved arctan function.

Now we consider the case where $m_d \neq 0$. By Theorem 5, the threshold for persistence of a population in a domain of length L occurs when $R_0 = 1$. Recall that by Corollary 7, R_0 is the principal eigenvalue of the next generation operator associated with (5.1). Alternatively, one can find R_0 by solving the eigenvalue problem

$$
\frac{f}{m_b + \mu}\varphi(x) + \frac{f\sigma\mu}{(m_b + \mu)^2}\int_0^L k(x,y)\varphi(y)\,dy = \lambda\varphi(x). \tag{5.3}
$$

Applying the linear operator $\mathcal{L}$ to (5.3), we obtain a Sturm–Liouville problem. Then by choosing $\lambda = R_0 = 1$ and finding the minimum positive solution of the Sturm–Liouville problem, we see that $f \le m_b + \mu$ and $v < 2\sqrt{D[\sigma\mu/(m_b + \mu - f) - \sigma - m_d]} := c^*$ are necessary

conditions for the population to persist, and when $v < c^*$, the critical domain size under hostile boundary conditions (2.2) is given by

(5.4)
$$L_{\text{crit}} = \frac{2D}{\sqrt{4D\left(\frac{\sigma\mu}{m_b+\mu-f} - \sigma - m_d\right) - v^2}} \left(\pi - \arctan\left(\sqrt{\frac{4D}{v^2}\left(\frac{\sigma\mu}{m_b+\mu-f} - \sigma - m_d\right) - 1}\right)\right),$$

which is equivalent to L_{crit} in (5.2) when $m_d = 0$. A full calculation in provided in Appendix B.

Similar calculations show when $v < c^*/\sqrt{2}$, the critical domain size for (5.1) under Danckwert's boundary conditions (2.3) is given by

$$L_{\text{crit}}^{\text{Dan}} = \frac{2D}{\sqrt{4D\left(\frac{\sigma\mu}{m_b+\mu-f} - \sigma - m_d\right) - v^2}} \arctan\left(\frac{\sqrt{\frac{4D}{v^2}\left(\frac{\sigma\mu}{m_b+\mu-f} - \sigma - m_d\right) - 1}}{\frac{2D}{v^2}\left(\frac{\sigma\mu}{m_b+\mu-f} - \sigma - m_d\right) - 1}\right). \tag{5.5}$$

When $c^*/\sqrt{2} < v < c^*$, the critical domain size is

(5.6)
$$L_{\text{crit}}^{\text{Dan}} = \frac{2D}{\sqrt{4D\left(\frac{\sigma\mu}{m_b+\mu-f} - \sigma - m_d\right) - v^2}} \left(\pi - \arctan\left(\frac{\sqrt{\frac{4D}{v^2}\left(\frac{\sigma\mu}{m_b+\mu-f} - \sigma - m_d\right) - 1}}{1 - \frac{2D}{v^2}\left(\frac{\sigma\mu}{m_b+\mu-f} - \sigma - m_d\right)}\right)\right).$$

6. Comparison between the benthic-drift model and the single compartment model.

In this section, we compare the benthic-drift model (2.1) the single compartment model (1.1) in [22] from the perspectives of model formulations, theoretical analysis, numerical methods, and biological applications.

6.1. Difference between the model formulations.

The single compartment model (1.1) assumes a single population, dispersing and reproducing in the flow. The benthic-drift model (2.1) assumes separate flow and benthic compartments with reproduction in the benthic compartment and transfer back and forth between compartments.

6.2. Theory difference between two models.

In both [22] and the current work, we define three measures of persistence, R_{loc}, R_δ, and R_0, in the context of a next generation operator Γ; our goal is to derive a useful persisence threshold and to use it to determine how population persistence/extinction depends on biotic and abiotic factors in the system.

Model (1.1) is a standard parabolic equation. The existence of the principal eigenvalue of the eigenvalue problem associated with the linearized system of (1.1) has been well established and it has been proved that this principal eigenvalue can be used to predict the stability of the trivial steady state (see e.g., [5, 26]). The solution map of the model and the resultant next generator operator are both compact. Hence, a theory of an infinite-dimensional dynamics system in [29] can be applied to establish the net reproductive rate.

Model (2.1) is a system consisting of a parabolic equation and an ordinary differential equation and there is clearly no diffusion term in the ordinary differential equation. The

solution maps are hence not compact. There is no standard theory for the principal eigenvalue of the associated eigenvalue problem in the case where parameters are spatial or time varying; see, e.g., [3, 15, 16] for similar systems with constant coefficients. Therefore we have to address the existence of the principal eigenvalue of the associated eigenvalue problem (see a recent theory in [31]) and establish the result that it can be used to determine the stability of the trivial steady state. In the most general case where all parameters vary, the next generation operator is not compact. Even though we can still use the theory in [29] to define the spectral radius of the next generation operator as the net reproductive rate for prediction of population persistence, we cannot show that the net reproductive rate is the principal eigenvalue of the next generation operator.

6.3. Difference in numerically computing R_0. For the single compartment model (1.1) studied in [22], the compactness of Γ_1 guarantees that R_0 is the dominant eigenvalue of Γ_1, hence R_0 can be found by solving the eigenvalue problem

$$\Gamma_1 \phi = R_0 \phi, \tag{6.1}$$

where $\phi(x)$ is the positive function associated with the dominant eigenvalue R_0 of the operator Γ_1. In most cases, it is not possible to find an analytic expression for R_0. A projection method was used in [22] for numerically approximating R_0. By using the projection method, the eigenvalue problem (6.1) was approximated by a matrix eigenvalue problem

$$\Gamma_{1,n} \phi_n = R_{0,n} \phi_n, \tag{6.2}$$

where $\Gamma_{1,n}$ is an $n \times n$ matrix and ϕ_n is an n-dimensional vector. Thus, R_0 can be approximated by the dominant eigenvalue of $\Gamma_{1,n}$ for very large n.

In this work, to calculate R_0, we introduced a new operator $\hat{\Gamma} : X \to X$, which has the same spectral radius as $\Gamma : X \times X \to X \times X$, to simplify the calculation of R_0. However, the operator $\hat{\Gamma}$ is still not compact due to the first term of the right side of (3.14), the Krein–Rutman theorem does not apply, the spectral radius of $\hat{\Gamma}$ may not be an eigenvalue of $\hat{\Gamma}$. Therefore, we approximated R_0 (the spectral radius of $\hat{\Gamma}$) by the spectral radius of a sufficiently large matrix (see section 3.4.3).

6.4. Effect of benthic zone on population persistence. We now examine the effect of the benthic compartment on population persistence. To do this, we compare the critical domain size for the benthic-drift model (5.1) to the critical domain sizes for two related single compartment population models under hostile boundary conditions. The critical domain size for the benthic-drift model (5.1) with hostile boundary conditions L_{crit} is given by (5.4).

First, we assume that the population has the same birth rate and death rate as in (5.1), is subjected to the same flow condition as in (5.1), but only lives in the flowing water and does not settle down to the benthos. The population dynamics can be described by the following model

$$\frac{\partial N}{\partial t} = gN - v\frac{\partial N}{\partial x} + D\frac{\partial^2 N}{\partial x^2}, \tag{6.3}$$

where $g = f - m$. We denote the critical domain size for (6.3) by $L_{\text{crit}}^{\text{single}}$. By using (3.10) in [22], we obtain

$$L_{\text{crit}}^{\text{single}} = \frac{1}{\sqrt{\frac{f-m}{D} - (\frac{v}{2D})^2}} \left(\arctan\left(-\frac{2D\sqrt{\frac{f-m}{D} - (\frac{v}{2D})^2}}{v} \right) + \pi \right). \tag{6.4}$$

Second we consider a limiting transfer case of system (5.1). When the transfer between the benthic and drift components of the population occurs on a fast timescale ($\sigma, \mu \to \infty$ with $\sigma = c\mu$, c is a constant). Since $\mu \to \infty$, the second equation of (5.1) yields $N_b = cN_d$. Summing the first and second equations of (5.1) we obtain the following single-compartment model:

$$\frac{\partial N_d}{\partial t} = \tilde{g} N_d - \tilde{v} \frac{\partial N_d}{\partial x} + \tilde{D} \frac{\partial^2 N_d}{\partial x^2} \tag{6.5}$$

with

$$\tilde{g} = \frac{c}{1+c} f - \frac{cm_b + m_d}{1+c}, \quad \tilde{v} = \frac{v}{1+c}, \quad \text{and} \quad \tilde{D} = \frac{D}{1+c}. \tag{6.6}$$

We denote the critical domain size for (6.5) by $L_{\text{crit}}^{\text{limit}}$. By using (3.10) in [22] again, we can obtain

$$L_{\text{crit}}^{\text{limit}} = \frac{1}{\sqrt{\frac{c(f-m_b)-m_d}{D} - (\frac{v}{2D})^2}} \left(\arctan\left(-\frac{2D\sqrt{\frac{c(f-m_b)-m_d}{D} - (\frac{v}{2D})^2}}{v} \right) + \pi \right). \tag{6.7}$$

By using (5.4), (6.4), and (6.7), we can compare the critical domain sizes for (5.1), (6.3), and (6.5). Let $\sigma = c\mu$ in (5.4). Then

$$\begin{aligned} L_{\text{crit}} &= \frac{2D}{\sqrt{4D\left(\frac{-c\mu m_b + c\mu f}{m_b + \mu - f} - m_d\right) - v^2}} \left(\pi - \arctan \sqrt{\frac{4D}{v^2}\left(\frac{-c\mu m_b + c\mu f}{m_b + \mu - f} - m_d\right) - 1} \right) \\ &= \frac{2D}{\sqrt{4D\left(\frac{-cm_b + cf}{\frac{m_b}{\mu} + 1 - \frac{f}{\mu}} - m_d\right) - v^2}} \left(\pi - \arctan \sqrt{\frac{4D}{v^2}\left(\frac{-cm_b + cf}{\frac{m_b}{\mu} + 1 - \frac{f}{\mu}} - m_d\right) - 1} \right) \\ &\to \frac{2D}{\sqrt{4D\left(-cm_b + cf - m_d\right) - v^2}} \left(\pi - \arctan \sqrt{\frac{4D}{v^2}(-cm_b + cf - m_d) - 1} \right), \end{aligned}$$

as $\mu \to \infty$. We note that this limiting value of L_{crit} is identical to $L_{\text{crit}}^{\text{limit}}$. This implies

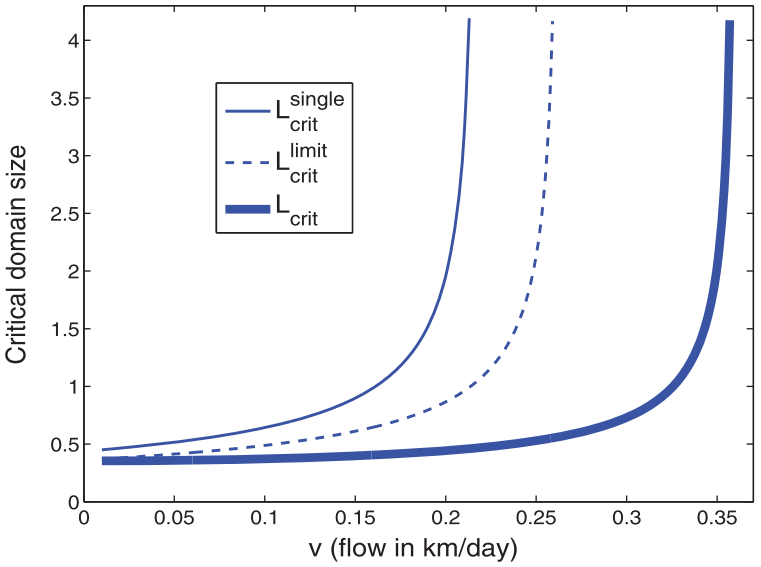

Figure 7. *Comparison of critical domain size for the single compartment model (L_{crit}^{single}), critical domain size for the limiting case of the benthic-drift model (L_{crit}^{limit}), and critical domain size for the benthic-drift model (L_{crit}). The model parameters are $D = 0.35\ m^2/s$, $g = f - m = 0.39\ day^{-1}$, $\sigma = 2\ day^{-1}$, and $\mu = 1\ day^{-1}$.*

that when the transfer rates are very large, the single compartmental model (6.5) can be used to predict the long-term dynamics of the benthic-drift model (5.1). Moreover, in the case where the mortality rates $m_b = m_d = m$, we observe that $L_{\text{crit}} = L_{\text{crit}}^{\text{single}}$ if and only if $\sigma(f-m)/(m+\mu-f) = f$, which indicates that if the mortality rate is the same on the benthos or in the drifting water, then population persistence/extinction of (5.1) can be predicted by (6.3) only if the transfer rates satisfy certain conditions.

We then compare the dependence of $L_{\text{crit}}^{\text{single}}$, $L_{\text{crit}}^{\text{limit}}$, and L_{crit} on the flow velocity v (Figure 7). For simplicity, we assume that $m_d = m_b = m$. The dependence of $L_{\text{crit}}^{\text{single}}$ on flow velocity was shown in [22] by choosing $D = 0.35\ m^2/s$, $g = f - m = 0.39\ \text{day}^{-1}$ (see Figure 3.1 in [22]). Here we choose the same values of D and g. We choose $\sigma = 2\ \text{day}^{-1}$ and $\mu = 1\ \text{day}^{-1}$ (hence $c = 2$) to calculate L_{crit} and $L_{\text{crit}}^{\text{limit}}$.

Figure 7 shows that the critical domain sizes are increasing functions of v, and at critical values of v, the critical domain sizes become infinite. If we denote the critical values of flow velocity at which $L_{\text{crit}}^{\text{single}}$, $L_{\text{crit}}^{\text{limit}}$, and L_{crit} are infinity by v_*^{single}, v_*^{limit}, and v_*, respectively, then $v_*^{\text{single}} < v_*^{\text{limit}} < v_*$. Moreover, when $v < v_*^{\text{single}}$, $L_{\text{crit}}^{\text{single}}(v) > L_{\text{crit}}^{\text{limit}}(v) > L_{\text{crit}}(v)$. These indicate that both single compartmental models overestimate the critical domain size for the benthic-drift model, or underestimate the persistence situation of a population in a benthic-drift environment. This also implies that the benthic component has a positive effect on the ability of the population to persist in a river with a finite length.

7. Discussion. In this paper, we considered persistence of a population in a stream described by the benthic-drift model (2.1) where the stream was divided into two zones (drifting zone and storage zone) and the population was divided into two interacting groups. The model (2.1) is a natural extension of the reaction-diffusion-reaction model (1.1) studied in

[22] for a single population. It can better describe the dynamics of species, such as some invertebrates, which spend most of the time living on the benthos but occasionally jump into the drifting water and disperse. Theoretically, we extended the three measures of population persistence, $R_{\text{loc}}(x)$, $R_\delta(x)$, and R_0, which were initially proposed in [19] and then studied for model (1.1) in [22], to our benthic-drift model. These measures were introduced in the context of a next generation operator based on the linearization of (2.1). Using the results of [31] we proved that R_0 determines the stability of the trivial homogeneous steady state of the nonlinear model (2.1). Thus, R_0 determined whether a population is able to persist in the stream or not.

To numerically calculate R_0, we defined a new operator $\hat{\Gamma}$ that is not related to a time-dependent problem and is only defined in the continuous function space but not the function vector space. We proved that $\hat{\Gamma}$ and the next generation operator Γ have the same spectral radius R_0. In fact, $\hat{\Gamma}$ can be thought of as playing the following role: if a population is initially distributed on the benthos, undergoes continuous transfer between the benthic zone and the drifting zone, disperses in the drift, and reproduces on the benthos, then the operator $\hat{\Gamma}$ maps the initial population distribution on the benthos to the distribution of the offspring produced by that population on the benthos over its lifetime. Based on the operator $\hat{\Gamma}$, we developed a numerical scheme using a collocation method for computing R_0 and R_δ.

We investigated how the interaction between flow speed and settling rate affects the population persistence by numerically calculating R_δ and R_0. In particular, we studied a model where the birth rate increases linearly downstream. When the environment was variable we found by using $R_\delta(x)$ that both the upstream boundary and the downstream boundary affected the size and the distribution of source-sink regions. In the upstream, the birth rate is smaller than the mortality rate, the upstream of the stream acts as a sink. This upstream effect is mitigated by increasing flow speed, as it carried individuals downstream to better habitat. The downstream effects include loss of individuals especially when allowing for hostile boundary conditions, and the positive growth rate associated with good primary productivity in the downstream reaches of the stream. Thus, increasing flow negatively affects the population persistence by increasing the loss of individuals, but positively affects the population persistence by carrying more individuals downstream where they can achieve a higher growth rate. Both such negative and positive effects can be mitigated by increasing the settling rate. It would be interesting to consider a spatially variable settling rate driven by the flow or somehow by the individuals' intention of escaping from washout.

Equation (3.16) shows that, once the area of the drift zone A_d is fixed, then for any constant area of the benthic zone A_b, we obtain the same net reproductive rate R_0. In this situation, the long term persistence dynamics of the population does not depend on how large the benthic zone is. However, if the benthic zone is heterogenous, as discussed in section 4.4, the population persistence significantly depends on the distribution of shallows and deep pools in a river. In this situation, deep pools in the upstream provide shelters which prevent individuals from being carried to the downstream and being washed out.

We applied R_0 theory to find the critical domain size for the benthic-drift model. We then compared the critical domain size for the benthic-drift model and two related single compartmental models and showed that in a limited case when the transfer rates approach infinity, a single compartment can be used to predict the long-term persistence behavior of a

population living in a benthic-drift habitat. Numerical simulations also verified that a benthic zone helps population persist in a river.

The results for the critical domain size were based on the assumption that the river is homogenous. It would be interesting to further investigate how the critical domain size depends on the river heterogeneity. This would extend the theory of critical domain size in [20]. Therein, by dividing a river into alternating good and bad patches, the minimum length that supports a population was analyzed based on a one compartment model of the form (1.1). In addition, the living environment for aquatic species in streams or rivers can vary seasonally. The theory developed here could be extended to more general models by including the seasonal variations in population growth [14, 17] and the temporal variation of flow velocity [13].

As for the persistence condition for model (2.1), we have the following observation. If $f(x,0) - m_b(x) - \mu(x) > 0$ for some $x \in (0,L)$, then there exists some $\delta_x > 0$ such that for $N_b \in (0,\delta_x)$ we have $f(x,N_b) - m_b(x) - \mu(x) > 0$. This, together with the differential inequality

$$\frac{\partial N_b}{\partial t} \geq (f(x,N_b) - m_b(x) - \mu(x))N_b,$$

implies that $\liminf_{t\to\infty} N_b(x,t) \geq \epsilon_x > 0$ with some $\epsilon_x > 0$, regardless of the initial data, which, by our definition of persistence (3.4) means that the population persists in a long term. This indicates that if the birth rate is greater than the sum of the mortality rate and the transfer rate from the benthos to the water, then the population is guaranteed to persist. On the other hand, if we are only interested in persistence conditions for the model (2.1), we may assume without loss of generality that $f(x,0) - m_b(x) - \mu(x) \leq 0$ for all $x \in (0,L)$.

Our model (2.1) is a system consisting of a parabolic equation and an ordinary differential equation. It is not the first time this type of system has been studied. Similar models have been proposed to describe microbial growth (see, e.g., [3, 15, 16]) and disease transmission (see, e.g., [31]), to name a few areas. Due to the lack of the diffusion in some of the equations, the solution maps are not compact, and hence, the study of such models are, in some sense, more difficult than that of standard parabolic systems. Smith and his collaborators in [3, 15, 16] considered microbial growth for limiting nutrient in a plug flow reactor with wall attachment in the one-dimensional space [3] and in the three-dimensional space [15, 16]. In such models, the bacteria suspended in the fluid and the wall-attached bacteria are similar to the drifting population and the benthic population, respectively, in our benthic-drift model (2.1). Based on some disease transmission models, Wang and Zhao [31] developed some nice general theory for the principal eigenvalue of the eigenvalue problem associated with a reaction-diffusion system where some of the diffusion terms are zeros. In this paper we adapt their theory to our benthic-drift river population model and develop persistence theories for our interest.

Our future plans include extending the theory and method of persistence measures in this paper to a two-dimensional benthic-drift model, which also allows spatial heterogeneity. Since we have the ability to incorporate a population model with a hydrological model in a numerical environment in River 2D [13], we plan to develop a numerical program in River 2D to calculate persistence measures for the two-dimensional population model. We expect that such a program can be directly used by ecologists or environmental managers.

Appendix A. Proofs.

A.1. Proof of Theorem 3. Let $\phi = (\phi_1, \phi_2) \in \bar{X}$, $\theta_1 = \min_{x\in[0,L]}\{f(x,0)-\mu(x)-m_b(x)\}$, and $\theta_2 = \max_{x\in[0,L]}\{f(x,0) - \mu(x) - m_b(x)\}$. From the second equation of (3.13), we have

$$\phi_2 = \frac{A_d(x)\sigma(x)}{A_b(x)(\lambda - f(x,0) + \mu(x) + m_b(x))}\phi_1. \tag{A.1}$$

Following Lemma 4.1 in [31], we define the linear operator $\mathcal{L}_\lambda$ as

$$\mathcal{L}_\lambda\phi = \mathcal{L}\phi - (\sigma(x) + m_d(x))\phi + \frac{\mu(x)\sigma(x)\phi}{\lambda - f(x,0) + \mu(x) + m_b(x)}, \quad \lambda > \theta_1. \tag{A.2}$$

Since $\mu(x)\sigma(x) \geq 0$ and $\mu(x)\sigma(x) \not\equiv 0$, there exists an interval $[x_1, x_2] \in (0, L)$ such that $\mu(x)\sigma(x) > 0$ for all $x \in [x_1, x_2]$. Let $\theta_0 = \min_{x\in[x_1,x_2]} \mu(x)\sigma(x)$ and let λ_1 be the principal eigenvalue of

$$\begin{cases} \mathcal{L}\phi - (\sigma(x) + m_d(x))\phi = \lambda\phi, & x \in (x_1, x_2), \\ \phi(x_1) = \phi(x_2) = 0, \end{cases} \tag{A.3}$$

with a positive eigenfunction $\phi^*(x)$. Then $\lambda_1 < 0$ (see Appendix A.6 in [22]). Set

$$\lambda_0 = \frac{k\lambda_1 + \theta_2 + \sqrt{(k\lambda_1 - \theta_2)^2 + 4\theta_0}}{2} \tag{A.4}$$

for some $k > 0$ such that

$$\lambda_1 + \frac{\theta_0}{\lambda_0 - \theta_1} \geq k\lambda_1 + \frac{\theta_0}{\lambda_0 - \theta_2}.$$

The choice of k is possible since $\lambda_1 < 0$. Then $\lambda_0 \geq \theta_2$ and

$$\begin{aligned} \mathcal{L}_{\lambda_0}\phi^*(x) &= \mathcal{L}\phi^*(x) - (\sigma(x) + m_d(x))\phi^*(x) + \frac{\mu(x)\sigma(x)\phi^*(x)}{\lambda_0 - f(x,0) + \mu(x) + m_b(x)} \\ &\geq \lambda_1\phi^*(x) + \frac{\theta_0\phi^*(x)}{\lambda_0 - \theta_1} \\ &\geq k\lambda_1\phi^*(x) + \frac{\theta_0\phi^*(x)}{\lambda_0 - \theta_2} \\ &= \lambda_0\phi^*(x) \quad \forall\, x \in (x_1, x_2). \end{aligned} \tag{A.5}$$

Now we define a continuous function $\phi_0(x)$ on $[0, L]$ by

$$\phi_0(x) = \begin{cases} \phi^*(x) & \text{if} \quad x \in [x_1, x_2], \\ 0 & \text{if} \quad x \in [0, L] \setminus [x_1, x_2]. \end{cases} \tag{A.6}$$

Then we have $\mathcal{L}_{\lambda_0}\phi_0(x) \geq \lambda_0\phi_0(x)$ $\forall x \in (0, L) \setminus \{x_1, x_2\}$. Consequently, $e^{\lambda_0 t}\phi_0(x, y)$ is a subsolution of the integral form of the linear system $u_t = \mathcal{L}_{\lambda_0}u$. By Theorem 2.3 and Remarks 2.1 and 2.2 in [31], problem (3.13) has an eigenvalue with geometric multiplicity one and a nonnegative eigenfunction. In terms of (3.13) and its associated parabolic system, we can easily see that this eigenfunction is positive.

A.2. Proof of Theorem 5. The proof of (i) is similar to that of Theorem 3.1(ii) in [31], hence it is omitted. To prove statement (ii), we first note that by Lemma 4, if $R_0 > 1$, then $\lambda^* > 0$. Similarly as in Theorem 3, we can prove that for sufficiently small $\epsilon > 0$, the eigenvalue problem

$$
\text{(A.7)}\quad \begin{cases} \dfrac{A_b(x)}{A_d(x)}\mu(x)N_b - \sigma(x)N_d - m_d(x)N_d + \mathcal{L}N_d = \lambda N_d, \quad x \in (0,L), t > 0, \\ (f(x,0)-\epsilon)N_b - m_b(x)N_b - \mu(x)N_b + \dfrac{A_d(x)}{A_b(x)}\sigma(x)N_d = \lambda N_b, \quad x \in (0,L), t > 0, \\ \alpha_1 N_d(0,t) - \beta_1 \dfrac{\partial N_d}{\partial x}(0,t) = 0, \quad t > 0, \\ \alpha_2 N_d(L,t) + \beta_2 \dfrac{\partial N_d}{\partial x}(L,t) = 0, \quad t > 0, \end{cases}
$$

admits a principal eigenvalue λ_ϵ^* with a positive eigenfunction $\phi_\epsilon^*(x)$.

Claim. $\lambda_\epsilon^* \to \lambda^*$ as $\epsilon \to 0$.

We can follow the proof of [31, Theorem 2.3] to prove this claim. Let $M_{11}(x) = -\sigma(x) - m_d(x)$, $M_{12}(x) = \mu(x)A_b(x)/A_d(x)$, $M_{21}(x) = \sigma(x)A_d(x)/A_b(x)$, $M_{22}(x) = f(x,0) - \epsilon - m_b(x) - \mu(x)$, $\theta_\epsilon = \max_{x\in[0,L]}\{M_{22}(x)\}$. It follows from [29, Theorem 3.12] that

$$
(\lambda - M_{22})^{-1}N_b = \int_0^\infty e^{-\lambda t}e^{M_{22}t}N_b dt
$$

for all $\lambda > \theta_\epsilon$. Let

$$
\mathcal{L}_{\lambda,\epsilon} = \mathcal{L} + M_{11} + M_{12}(\lambda - M_{22}(x))^{-1}M_{21} \ \forall \lambda > \theta_\epsilon.
$$

For any $\lambda > \theta_\epsilon$, let $T_{\lambda,\epsilon}(t)$ be the semigroup generated by $\mathcal{L}_{\lambda,\epsilon}$ and define $\zeta(\lambda,\epsilon) = s(\mathcal{L}_{\lambda,\epsilon})$, the spectral bound of $\mathcal{L}_{\lambda,\epsilon}$. Then $T_{\lambda,\epsilon}$ is a compact and strongly positive operator for each $t > 0$ (see, e.g., the proof of [26, Theorem 7.5.1]). By [31, Theorem 2.2], $\zeta(\lambda,\epsilon)$ is the principal eigenvalue of $\mathcal{L}_{\lambda,\epsilon}$. By the continuity of a finite system of eigenvalues (see [18, section IV.3.5]), it follows that $\zeta(\lambda,\epsilon)$ is a continuous function in λ and ϵ for $\lambda > \theta_\epsilon$ and small ϵ. Let $G(\lambda,\epsilon) = \zeta(\lambda,\epsilon) - \lambda$. Similarly as in the proof of Theorem 3, we can show that there exists $\lambda_0 > \theta_\epsilon$ and $\phi_0 > 0$ such that $\mathcal{L}_{\lambda_0,\epsilon}\phi_0 \geq \lambda_0\phi_0$. Then by similar arguments as in the proof of [31, Theorem 2.3], we can obtain that $\zeta(\lambda_0,\epsilon) \geq \lambda_0$ for any given small $\epsilon > 0$, and furthermore, there is a unique $\lambda_\epsilon^* > \theta_\epsilon$ such that $G(\lambda_\epsilon^*,\epsilon) = 0$, i.e., $\zeta(\lambda_\epsilon^*,\epsilon) = \lambda_\epsilon^*$. Moreover, λ_ϵ^* is the principal eigenvalue of (A.7) with a positive eigenvector. It then follows from the continuity of ζ in λ and ϵ that the principal eigenvalue λ_ϵ^* of (A.7) is a continuous function of ϵ, and hence, $\lambda_\epsilon^* \to \lambda^*$ as $\epsilon \to 0$. The claim is proved.

Since $\lambda_\epsilon^* \to \lambda^*$ as $\epsilon \to 0$ and $\lambda^* > 0$, there exists a small $\bar{\epsilon} > 0$ such that $\lambda_\epsilon^* > 0$ for all $\epsilon \in (0,\bar{\epsilon})$. Take $\epsilon_0 \in (0,\bar{\epsilon})$. By the continuity of f, there exists a $\delta > 0$ such that $|f(x,N_b) - f(x,0)| < \epsilon_0$ when $N_b < \delta$ for all $x \in [0,L]$. Assume, for the sake of contradiction, that there exists a positive solution $(N_d(x,t), N_b(x,t))$ of (2.1) such that

$$
\text{(A.8)}\qquad \limsup_{t\to\infty} ||(N_d(x,t), N_b(x,t) - (0,0)||_\infty < \delta.
$$

Then there exists a large $t_0 > 0$, such that $N_b(x,t) < \delta$ and $f(x, N_b(x,t)) > f(x,0) - \epsilon_0$ for all $x \in [0,L]$ and $t \geq t_0$. Therefore,

$$\text{(A.9)} \quad \begin{cases} \dfrac{\partial N_d}{\partial t} = \dfrac{A_b(x)}{A_d(x)}\mu(x)N_b - \sigma(x)N_d - m_d(x)N_d + \mathcal{L}N_d, & x \in (0,L), \\ \dfrac{\partial N_b}{\partial t} \geq (f(x,0) - \epsilon_0)N_b - m_b(x)N_b - \mu(x)N_b + \dfrac{A_d(x)}{A_b(x)}\sigma(x)N_d, & x \in (0,L), \end{cases}$$

for all $t \geq t_0$. Since $N_d(t_0,x) \gg 0, N_b(t_0,x) \gg 0$ in the interior of $[0,L]$, we can choose a sufficiently small number $\eta > 0$, such that $(N_d(t_0,\cdot), N_b(t_0,\cdot)) \geq \eta\phi^*_{\epsilon_0}(\cdot)$, where $\phi^*_{\epsilon_0}(\cdot)$ is the positive eigenfunction of (A.7) (with $\epsilon = \epsilon_0$) corresponding to $\lambda^*_{\epsilon_0}$. Note that $\eta e^{\lambda^*_{\epsilon_0}(t-t_0)}\phi^*_{\epsilon_0}(x)$ is a solution of

$$\text{(A.10)} \quad \begin{cases} \dfrac{\partial N_d}{\partial t} = \dfrac{A_b(x)}{A_d(x)}\mu(x)N_b - \sigma(x)N_d - m_d(x)N_d + \mathcal{L}N_d, & x \in (0,L), \\ \dfrac{\partial N_b}{\partial t} = (f(x,0) - \epsilon_0)N_b - m_b(x)N_b - \mu(x)N_b + \dfrac{A_d(x)}{A_b(x)}\sigma(x)N_d, & x \in (0,L), \end{cases}$$

for $t \geq t_0$. Then the comparison principle implies $(N_d(x,t), N_b(x,t)) \geq \eta e^{\lambda^*_{\epsilon_0}(t-t_0)}\phi^*_{\epsilon_0}(x)$ $\forall x \in [0,L], t \geq t_0$, and hence, $\max_{x\in[0,L]} N_d(x,t) \to \infty$ and $\max_{x\in[0,L]} N_b(x,t) \to \infty$ as $t \to \infty$, which contradicts (A.8). This proves statement (ii).

A.3. Proof of Theorem 6.

Let

$$\mathcal{B} = \begin{pmatrix} -\sigma(x) - m_d(x) + \mathcal{L} & \dfrac{A_b(x)}{A_d(x)}\mu(x) \\ \dfrac{A_d(x)}{A_b(x)}\sigma(x) & -\mu(x) - m_b(x) \end{pmatrix}, \mathcal{F}(x) = \begin{pmatrix} 0 & 0 \\ 0 & f(x,0) \end{pmatrix}, \mathcal{V} = \begin{pmatrix} \mathcal{L} & 0 \\ 0 & 0 \end{pmatrix} - \mathcal{B}.$$

Let $T(t)$ be the solution semigroup on $X \times X$ associated with system (3.2). Then $\mathcal{B}$ is the generator of $T(t)$ on $X \times X$ and $T(t)$ is a positive semigroup in the sense that $T(t)(X_+ \times X_+) \subseteq (X_+ \times X_+)$ for all $t \geq 0$. It then follows from [29, Theorem 3.12] that $\mathcal{B}$ is resolvent positive and

$$(\lambda I - \mathcal{B})^{-1}\phi = \int_0^\infty e^{-\lambda t}T(t)\phi\, dt \text{ for all } \lambda > s(\mathcal{B}) \text{ and } \phi \in X \times X,$$

where $s(\mathcal{B}) = \sup\{\text{Re}\,\lambda : \lambda \in \sigma(\mathcal{B})\}$ is the spectral bound of $\mathcal{B}$. Note that [31, Theorem 2.3] implies that $s(\mathcal{B}) < 0$. Then for $\lambda = 0$ we have

$$-\mathcal{B}^{-1}\phi = \int_0^\infty T(t)\phi dt \ \ \forall \phi \in X \times X.$$

This implies that $\Gamma = -\mathcal{F}\mathcal{B}^{-1}$ (see also, e.g., the proof of [31, Theorem 3.1]). It follows from the spectral radius formula that

$$r(-\mathcal{F}\mathcal{B}^{-1}) = \lim_{n\to\infty} ||(-\mathcal{F}\mathcal{B}^{-1})^n||^{\frac{1}{n}} = \lim_{n\to\infty} ||(-\mathcal{B}^{-1}\mathcal{F})^n||^{\frac{1}{n}} = r(-\mathcal{B}^{-1}\mathcal{F}).$$

Then we have

$$R_0 = r(\Gamma) = r(-\mathcal{F}\mathcal{B}^{-1}) = r(-\mathcal{B}^{-1}\mathcal{F}).$$

Let $\Lambda = -\mathcal{B}^{-1}\mathcal{F}$. For any $\phi = (\phi_1, \phi_2) \in X \times X$, let $\psi = (\psi_1, \psi_2) = \Lambda\phi$. Then $-\mathcal{B}\psi = -\mathcal{B}(-\mathcal{B}^{-1}\mathcal{F})\phi = \mathcal{F}\phi$. That is,

$$\begin{aligned} -\mathcal{L}\psi_1 + v_{11}\psi_1 + v_{12}\psi_2 &= 0, \\ v_{21}\psi_1 + v_{22}\psi_2 &= \mathcal{F}_{22}\phi_2, \end{aligned}$$

where $\mathcal{F}_{22} = f(x,0)$, $v_{11} = \sigma(x) + m_d(x)$, $v_{12} = -A_b(x)\mu(x)/A_d(x)$, $v_{21} = -A_d(x)\sigma(x)/A_b(x)$, $v_{22} = m_b(x) + \mu(x)$. Then $\psi_2 = v_{22}^{-1}(\mathcal{F}_{22}\phi_2 - v_{21}\psi_1)$, and hence,

$$-\mathcal{L}\psi_1 + v_{11}\psi_1 - v_{12}v_{22}^{-1}v_{21}\psi_1 = -v_{12}v_{22}^{-1}\mathcal{F}_{22}\phi_2.$$

Let

$$\mathcal{B}_1 := \mathcal{L} - v_{11} + v_{12}v_{22}^{-1}v_{21}, \quad \mathcal{B}_2 := \mathcal{B}_1^{-1}v_{12}v_{22}^{-1}\mathcal{F}_{22}, \quad \mathcal{B}_3 := v_{22}^{-1}\mathcal{F}_{22} - v_{22}^{-1}v_{21}\mathcal{B}_1^{-1}v_{12}v_{22}^{-1}\mathcal{F}_{22}.$$

Then

$$\psi_1 = \mathcal{B}_1^{-1}v_{12}v_{22}^{-1}\mathcal{F}_{22}\phi_2 = \mathcal{B}_2\phi_2, \quad \psi_2 = v_{22}^{-1}(\mathcal{F}_{22} - v_{21}\mathcal{B}_1^{-1}v_{12}v_{22}^{-1}\mathcal{F}_{22})\phi_2 = \mathcal{B}_3\phi_2.$$

Therefore,

$$\Lambda\phi = (\mathcal{B}_2\phi_2, \mathcal{B}_3\phi_2) \quad \forall \phi = (\phi_1, \phi_2) \in X \times X.$$

By induction, we obtain

$$\Lambda^n\phi = (\mathcal{B}_2\mathcal{B}_3^{n-1}\phi_2, \mathcal{B}_3^n\phi_2) \ \forall n \geq 2.$$

Thus,

$$||\mathcal{B}_3^n|| \leq ||\Lambda^n|| \leq (||\mathcal{B}_2||^2 \cdot ||\mathcal{B}_3^{n-1}||^2 + ||\mathcal{B}_3^n||^2)^{1/2} \ \forall n \geq 2,$$

and hence by the formula of the spectral radius, we obtain

$$R_0 = r(\Lambda) = \lim_{n\to\infty} ||\Lambda^n||^{\frac{1}{n}} = \lim_{n\to\infty} ||\mathcal{B}_3^n||^{\frac{1}{n}} = r(\mathcal{B}_3).$$

It follows from [22, Propositions 2.5 and 2.10] that for any $\varphi \in X$,

$$-\mathcal{B}_1^{-1}\varphi(x) = \int_0^L k(x,y)\varphi(y)\,dy, \tag{A.11}$$

where $k(x,y)$ is the solution of the ordinary boundary value problem

$$\begin{cases} \left(\mathcal{L} - \sigma(x) - m_d(x) + \dfrac{\sigma(x)\mu(x)}{m_b(x)+\mu(x)}\right)k(x,y) = -\delta(x-y),\ x \in (0,L), \\ \alpha_1 k(0,y) - \beta_1 \dfrac{\partial k}{\partial x}(0,y) = 0, \\ \alpha_2 k(L,y) + \beta_2 \dfrac{\partial k}{\partial x}(L,y) = 0 \end{cases} \tag{A.12}$$

for a fixed value of y. Then for any $\varphi \in X$,

$$[\mathcal{B}_3\varphi](x) = \frac{f(x,0)\varphi(x)}{m_b(x)+\mu(x)} + \frac{\sigma(x)A_d(x)}{(m_b(x)+\mu(x))A_b(x)}\int_0^L k(x,y)\frac{f(y,0)\mu(y)A_b(y)\varphi(y)}{(m_b(y)+\mu(y))A_d(y)}dy\,dy.$$

Let $\hat{\Gamma} = \mathcal{B}_3$. Then $R_0 = r(\Gamma) = r(\hat{\Gamma})$. The proof of Theorem 6 is completed.

A.4. Proof of Corollary 7. Note that $\hat{\Gamma} = a + b\Phi$, where $a := \frac{f}{m_b+\mu}$ and $b := \frac{\sigma\mu f}{(m_b+\mu)^2}$ for simplicity. This indicates that $\varsigma \in \sigma(\Phi)$ if and only if $\lambda = a + b\varsigma \in \sigma(\hat{\Gamma})$. Moreover, ς is an eigenvalue of Φ with associated eigenfunction $\varphi \in X$, i.e., $\Phi\varphi = \varsigma\varphi$, if and only if $\lambda = a+b\varsigma$ is an eigenvalue of $\hat{\Gamma}$ with the same associated eigenfunction φ, i.e., $\hat{\Gamma}\varphi = \lambda\varphi = (a+b\varsigma)\varphi$. Since the operator Φ is a continuous, strongly positive, compact, linear operator on X, its spectral radius, given by $\sup\{|\varsigma| : \varsigma \in \sigma(\Phi)\}$, is equal to its principal eigenvalue ς^*, which is the only eigenvalue of Φ with a positive eigenfunction $\varphi^* \in X$. Thus,

$$\begin{aligned} R_0 = r(\hat{\Gamma}) &= \sup\{|\lambda| : \lambda \in \sigma(\hat{\Gamma})\} = \sup\{|a + b\varsigma| : \varsigma \in \sigma(\Phi)\} \\ &\le a + b\sup\{|\varsigma| : \varsigma \in \sigma(\Phi)\} = a + b\varsigma^*. \end{aligned}$$

Note that $a + b\varsigma^*$ is an eigenvalue of $\hat{\Gamma}$ with associated eigenfunction φ^*, which implies that $a + b\varsigma^* \le R_0$. Therefore,

$$R_0 = r(\hat{\Gamma}) = a + b\varsigma^* = \frac{f}{m_b+\mu} + \frac{f\sigma\mu}{(m_b+\mu)^2}\varsigma^*.$$

Clearly, R_0 is the principal eigenvalue of $\hat{\Gamma}$ with a positive eigenfunction φ^*.

A.5. Proof of Proposition 8. Consider system (3.2) with initial condition

$$(n_d(x,0), n_b(x,0)) = (0, N_b^0(x)).$$

Integrating equations for n_d and n_b in (3.2) with respect to t from 0 to ∞ yields

$$\text{(A.13)} \quad \begin{cases} \displaystyle\int_0^\infty \frac{\partial n_d(x,t)}{\partial t}dt = \frac{\mu(x)}{\eta(x)}\int_0^\infty n_b(x,t)dt + (\mathcal{L} - \sigma(x) - m_d(x))\int_0^\infty n_d(x,t)dt, \\ \displaystyle\int_0^\infty \frac{\partial n_b(x,t)}{\partial t}dt = -(m_b(x)+\mu(x))\int_0^\infty n_b(x,t)dt + \eta(x)\sigma(x)\int_0^\infty n_d(x,t)dt, \end{cases}$$

where $\eta(x) = A_d(x)/A_b(x)$. Then

$$\text{(A.14)} \quad \begin{cases} \displaystyle 0 = \frac{\mu(x)}{\eta(x)}\int_0^\infty n_b(x,t)dt + (\mathcal{L} - \sigma(x) - m_d(x))\int_0^\infty n_d(x,t)dt, \\ \displaystyle -N_b^0(x) = -(m_b(x)+\mu(x))\int_0^\infty n_b(x,t)dt + \eta(x)\sigma(x)\int_0^\infty n_d(x,t)dt. \end{cases}$$

Therefore,

$$\text{(A.15)} \quad \int_0^\infty n_d(x,t)dt = \frac{(m_b(x)+\mu(x))\int_0^\infty n_b(x,t)dt - n_b^0(x)}{\sigma(x)\eta(x)} = \frac{(m_b(x)+\mu(x))G(x) - n_b^0(x)}{\sigma(x)\eta(x)},$$

where $G(x) := \int_0^\infty n_b(x,t)dt$. Hence,

$$\text{(A.16)} \quad 0 = \frac{\mu(x)}{\eta(x)}G(x) + (\mathcal{L} - \sigma(x) - m_d(x))\frac{(m_b(x)+\mu(x))G(x) - N_b^0(x)}{\sigma(x)\eta(x)},$$

which is equivalent to

(A.17)
$$\left(\mathcal{L}-\sigma(x)-m_d(x)+\frac{\sigma(x)\mu(x)}{m_b(x)+\mu(x)}\right)\frac{(m_b(x)+\mu(x))G(x)-N_b^0(x)}{\sigma(x)\eta(x)}=-\frac{\mu(x)N_b^0(x)}{(m_b(x)+\mu(x))\eta(x)}.$$

Let $k(x,y)$ be the solution of the following boundary value problem

(A.18)
$$\begin{cases}\left(\mathcal{L}-\sigma(x)-m_d(x)+\dfrac{\sigma(x)\mu(x)}{m_b(x)+\mu(x)}\right)k(x,y)=-\delta(x-y),\ x\in(0,L),\\ \alpha_1 k(0,y)-\beta_1\dfrac{\partial k}{\partial x}(0,y)=0,\\ \alpha_2 k(L,y)+\beta_2\dfrac{\partial k}{\partial x}(L,y)=0\end{cases}$$

for a fixed value of y. Thus,

(A.19)
$$\frac{(m_b(x)+\mu(x))G(x)-N_b^0(x)}{\sigma(x)\eta(x)}=\int_0^L k(x,y)\frac{\mu(y)N_b^0(y)}{(m_b(y)+\mu(y))\eta(y)}dy,$$

which implies that

(A.20)
$$G(x)=\int_0^\infty n_b(x,t)dt=\frac{N_b^0(x)}{m_b(x)+\mu(x)}+\frac{\sigma(x)\eta(x)}{m_b(x)+\mu(x)}\int_0^L k(x,y)\frac{\mu(y)N_b^0(y)}{(m_b(y)+\mu(y))\eta(y)}dy.$$

Let $N_b^0(\cdot)=\delta(\cdot-x_0)$ for a given point $x_0\in(0,L)$. By (A.20) and the definition of R_δ in (3.10), we obtain

$$\begin{aligned}R_\delta(x_0)&=\int_0^L f(z,0)\int_0^\infty n_b(z,t)dtdz\\&=\int_0^L f(z,0)\left(\frac{\delta(z-x_0)}{m_b(z)+\mu(z)}+\frac{\sigma(z)A_d(z)}{(m_b(z)+\mu(z))A_b(z)}\int_0^L k(z,y)\frac{\mu(y)\delta(y-x_0)A_b(y)}{(m_b(y)+\mu(y))A_d(y)}dy\right)dz\\&=\frac{f(x_0,0)}{m_b(x_0)+\mu(x_0)}+\frac{\mu(x_0)A_b(x_0)}{(m_b(x_0)+\mu(x_0))A_d(x_0)}\int_0^L f(z,0)k(z,x_0)\frac{\sigma(z)A_d(z)}{(m_b(z)+\mu(z))A_b(z)}dz.\end{aligned}$$

Appendix B. Calculation of critical domain size.

Setting

(B.1)
$$C_1=\frac{f}{m_b+\mu},\quad C_2=\frac{f\sigma\mu}{(m_b+\mu)^2},\quad C_3=\sigma+m_d-\frac{\sigma\mu}{m_b+\mu},$$

and applying the linear operator $\mathcal{L}-C_3$ to (5.3), we have

(B.2)
$$C_2\int_0^L\varphi(y)(\mathcal{L}-C_3)k(x,y)dy=(\lambda-C_1)(\mathcal{L}-C_3)\varphi(x).$$

Using the first equation of (3.15) we obtain

$$\varphi''(x) - \frac{v}{D}\varphi'(x) + \frac{1}{D}\left(\frac{C_2}{\lambda - C_1} - C_3\right)\varphi(x) = 0. \tag{B.3}$$

When $x = 0$, by (5.3) and the second equation of (3.15), we find

$$\alpha_1\varphi(0) - \beta_1\varphi'(0) = \frac{C_2}{\lambda - C_1}\int_0^L [\alpha_1 k(0,y) - \beta_1 k'(0,y)]dy = 0. \tag{B.4}$$

Similarly, by using (5.3) and the third equation of (3.15) we obtain

$$\alpha_2\varphi(L) + \beta_2\varphi'(L) = 0. \tag{B.5}$$

Thus, we consider the following Sturm–Liouville problem under the hostile boundary conditions

$$\begin{cases} \varphi''(x) - \dfrac{v}{D}\varphi'(x) + \dfrac{1}{D}\left(\dfrac{C_2}{\lambda - C_1} - C_3\right)\varphi(x) = 0, \quad x \in (0, L), \\ v\varphi(0) - D\varphi'(0) = 0, \quad \varphi(L) = 0. \end{cases} \tag{B.6}$$

The characteristic equation for (B.6) is

$$r^2 - \frac{v}{D}r + \frac{1}{D}\left(\frac{C_2}{\lambda - C_1} - C_3\right) = 0 \tag{B.7}$$

with discriminant

$$\Delta(\lambda) = \left(\frac{v}{D}\right)^2 - \frac{4}{D}\left(\frac{C_2}{\lambda - C_1} - C_3\right). \tag{B.8}$$

It is straightforward to show that (B.6) only has a zero solution when $\Delta \geq 0$. Thus, positive solutions of (B.6) exist only when $\Delta < 0$ or, equivalently, when

$$v < 2\sqrt{D\left(\frac{C_2}{\lambda - C_1} - C_3\right)}. \tag{B.9}$$

Notice that the population persistence in a domain of length L occurs when $\lambda = R_0 \geq 1$. If $\lambda \geq 1$, then (B.9) implies

$$v < 2\sqrt{D\left(\frac{C_2}{\lambda - C_1} - C_3\right)} \leq 2\sqrt{D\left(\frac{C_2}{1 - C_1} - C_3\right)} := c^*. \tag{B.10}$$

If $v > c^*$, then either (B.6) has no positive solution or a positive solution exists but $\lambda < 1$, which in either case implies that the zero solution is stable and the critical domain size does not exist. Thus $v < c^*$ is a necessary condition for the population to persist. If $v < c^*$, we choose $\lambda = R_0 = 1$, then (B.9) holds, hence (B.6) has positive solutions taking the form

$$\varphi(x) = \exp\left(\frac{v}{2D}x\right)\left[c_1 \cos\left(\frac{\sqrt{-\Delta(1)}}{2}x\right) + c_2 \sin\left(\frac{\sqrt{-\Delta(1)}}{2}x\right)\right], \tag{B.11}$$

where the constants c_1 and c_2 are determined by the boundary conditions.

To match the left-hand boundary condition, we now require

$$\frac{c_1}{c_2} = \frac{D}{v}\sqrt{-\Delta(1)}, \tag{B.12}$$

while matching the right-hand condition requires

$$\frac{c_1}{c_2} = -\tan\left(\frac{L}{2}\sqrt{-\Delta(1)}\right). \tag{B.13}$$

A solution matching both boundary conditions thus requires

$$\tan\left(\frac{L}{2}\sqrt{-\Delta(1)}\right) = -\frac{D}{v}\sqrt{-\Delta(1)}. \tag{B.14}$$

Therefore, if $v < c^*$, then the critical domain size L_{crit} is the minimum positive solution L of (B.14) given by

(B.15)

$$\begin{aligned} L_{\text{crit}} &= \frac{2}{\sqrt{-\Delta(1)}}\left(\pi - \arctan\left(\frac{D}{v}\sqrt{-\Delta(1)}\right)\right) \\ &= \frac{2D}{\sqrt{4D\left(\frac{\sigma\mu}{m_b+\mu-f} - \sigma - m_d\right) - v^2}}\left(\pi - \arctan\left(\sqrt{\frac{4D}{v^2}\left(\frac{\sigma\mu}{m_b+\mu-f} - \sigma - m_d\right) - 1}\right)\right). \end{aligned}$$

Acknowledgments. The authors are grateful to the anonymous referees for many insightful comments and references that helped improve the paper. The authors thank Lewis Lab for fruitful discussions.

REFERENCES

[1] J. D. Allan, *Stream Ecology: Structure and Function of Running Waters*, Chapman & Hall, London, 1995.

[2] K. E. Anderson, A. J. Paul, E. McCauley, L. J. Jackson, J. R. Post, and R. M. Nisbet, *Instream flow needs in streams and rivers: The importance of understanding ecological dynamics*, Front. Ecol. Enviro., 4 (2006), pp. 309–318.

[3] M. Ballyk and H. Smith, *A model of microbial growth in a plug flow reactor with wall attachment*, Math. Biosci., 158 (1999), pp. 95–126.

[4] K. E. Bencala and R. A. Walters, *Simulation of solute transport in a mountain poop-and-riffle stream: A transient storage model*, Water Res. Res., 19 (1983), pp. 718–724.

[5] R. S. Cantrell and C. Consner, *Spatial Ecology via Reaction-Diffusion Equation*, Wiley, Chichester, England, 2003.

[6] F. Chatelin, *The spectral approximation of linear operators with applications to the computation of eigenelements of differential and integral operators*, SIAM Rev., 23 (1981), pp. 495–522.

[7] D. L. DeAngelis, M. Loreaub, D. Neergaardc, P. J. Mulhollanda, and E. R. Marzolfa, *Modelling nutrient-periphyton dynamics in streams: The importance of transient storage zones*, Ecol. Model., 80 (1995), pp. 149–160.

[8] O. Diekmann, J. A. P. Heesterbeek, and J. A. J. Metz, *On the definition and the computation of the basic reproductive ratio r_0 in models for infectious diseases in heterogeneous populations*, J. Math. Biol., 28 (1990), pp. 365–382.

[9] Y. Du, *Order Structure and Topological Methods in Nonlinear Partial Differential Equations. Vol.* 1: *Maximum Principles and Applications*, Partial Differential Equations Appl. Ser. 2, World Scientific, River Edge, NJ, 2006.

[10] R. Guenther and J. Lee, *Partial Differential Equations of Mathematical Physics and Integral Equations*, Dover, New York, 1996.

[11] A. E. Hershey, J. Pastor, B. J. Peterson, and G. W. Kling, *Stable isotopes resolve the drift paradox for Baetis mayflies in an arctic river*, Ecology, 74 (1993), pp. 2315–2325.

[12] S.-B. Hsu, F.-B. Wang, and X.-Q. Zhao, *Global dynamics of zooplankton and harmful algae in flowing habitats*, J. Differential Equations., 255 (2013), pp. 265–297.

[13] Y. Jin, F. M. Hilker, P. M. Steffler, and Mark A. Lewis, *Seasonal invasion dynamics in a spatially heterogeneous river with fluctuating flows*, Bull. Math. Biol., 76 (2014), pp. 1522–1565.

[14] Y. Jin and M. A. Lewis, *Seasonal influences on population spread and persistence in streams: Critical domain size*, SIAM J. Appl. Math., 71 (2011), pp. 1241–1262.

[15] D. Jones, D. Le, H. Smith, and H. V. Kojouharov, *Bacterial wall attachment in a flow reactor*, SIAM J. Appl. Math., 62 (2002), pp. 1728–1771.

[16] D. Jones, H. V. Kojouharov, D. Le, and H. Smith, *The Freter model: A simple model of biofilm formation*, J. Math. Biol., 47 (2003), pp. 137–152.

[17] Y. Jin and M. A. Lewis, *Seasonal influences on population spread and persistence in streams: Spreading speeds*, J. Math. Biol., 65 (2012), pp. 403–439.

[18] T. Kato, *Perturbation Theory for Linear Operators*, Springer-Verlag, Berlin, 1976.

[19] M. Krkošek and M. A. Lewis, *An R_0 theory for source-sink dynamics with application to Dreissena competition*, Theoret. Ecol., 3 (2010), pp. 25–43.

[20] F. Lutscher, M. A. Lewis, and E. McCauley, *Effects of heterogeneity on spread and persistence in rivers*, Bull. Math. Biol., 68 (2006), pp. 2129–2160.

[21] R. Martin and H. L. Smith, *Abstract functional differential equations and reaction-diffusion systems*, Trans. Amer. Math. Soc., 321 (1990), pp. 1–44.

[22] H. W. McKenzie, Y. Jin, J. Jacobsen, and M. A. Lewis, *R_0 Analysis of a spatiotemporal model for a stream population*, SIAM J. Appl. Dyn. Syst., 11 (2012), pp. 567–596.

[23] P. J. Mulholland, A. D. Steinman, E. R. Marzolf, D. R. Hart, and D. L. DeAngelis, *Effect of periphyton biomass on hydraulic characteristics and nutrient cycling in streams*, Oecologia, 98 (1994), pp. 40–47.

[24] E. Pachepsky, F. Lutscher, R. M. Nisbet, and M. A. Lewis, *Persistence, spread and the drift paradox*, Theoret. Popul. Biol., 67 (2005), pp. 61–73.

[25] E. R. Siler, J. B. Wallace, and S. L. Eggert, *Long-term effects of resource limitation on stream invertebrate drift*, Canad. J. Fisheries Aquat. Sci., 58 (2001), pp. 1624–1637.
[26] H. L. Smith, *Monotone Dynamical Systems: An Introduction to the Theory of Competitive and Cooperative Systems*, in Math. Surveys Monogr. 41, AMS, Providence, RI, 1995.
[27] D. Speirs and W. Gurney, *Population persistence in rivers and estuaries*, Ecology, 82 (2001), pp. 1219–1237.
[28] I. Stakgold, *Green's Functions and Boundary Value Problems*, 2nd ed., Wiley, New York, 1998.
[29] H. R. Thieme, *Spectral bound and reproduction number for infinite-dimensional population structure and time heterogeneity*, SIAM J. Appl. Math., 70 (2009), pp. 188–211.
[30] F. J. Triska, J. H. Duff, and R. J. Avazino, *Influence of exchange flow between channel and hyporheic zone on nitrate production in a small mountain stream*, Canad. J. Fisheries Aquat. Sci., 47 (1990), pp. 2099–2111.
[31] W. Wang and X.-Q. Zhao, *Basic reproduction numbers for reaction-diffusion epidemic models*, SIAM J. Appl. Dyn. Syst., 11 (2012), pp. 1652–1673.